ADDIS ABABA UNIVERSITY

ADDIS ABABA INSTITUTE OF TECHNOLOGY

SCHOOL OF CHEMICAL AND BIO-ENGINEERING

Catalytic Oxidation of Phenol in Aqueous Solution using Fe - Sulfonated Carbon Catalyst

By: Tewodros Geremew

A Thesis submitted to

The School of Chemical and Bio Engineering, Addis Ababa Institute of Technology, Addis Ababa University

Presented in Partial Fulfilment of the Requirement for the Degree of Master of Science in Chemical Engineering (Environmental Engineering Stream)

Addis Ababa University

Addis Ababa, Ethiopia

July 2018

Addis Ababa University

Addis Ababa Institute of Technology

School of Chemical and Bio Engineering

This is to certify that the thesis prepared by Tewodros Geremew, entitled: "*catalytic oxidation of phenol in aqueous solution using Fe - sulfonated carbon catalyst"* and submitted in partial fulfilment of the requirement for the degree of Master of Science (Chemical and Bio Engineering) complies with the regulations of the university and meets the accepted standards with respect to originality and quality.

Signed by the Examining Committee:

Dr. Beteley Tekola (Assi. Prof.)	_____	July , 2018
Advisor	signature	Date
Dr. Shegaw Ahmed (Assi. Prof.)	_____	July , 2018
Internal Examiner	signature	Date
Prof. Belay Woldeyes.	_____	July , 2018
External Examiner	signature	Date

DECLARATION

I declare that this thesis entitled *"catalytic oxidation of phenol in aqueous solution using Fe - sulfonated carbon catalyst* " has not been submitted in any form for another degree, diploma or an award at any university or other institution of the tertiary education. Whenever contributions of others are involved, every effort is made to indicate this clearly, with due reference to the literature and discussions. Information taken from published and unpublished work of others has been acknowledged in the text and a list of references is given. The work was under the guidance of Dr. Beteley T. (Assistant Professor) instructor in Addis Ababa University, School of Chemical and Bio Engineering.

Name: Tewodros Geremew

Signature: _____

Date of Submission: July 2018

ABSTRACT

The main objective of this research was to mineralize phenol in aqueous solution using Fe – Sulfonated carbon catalyst. Two fairly different catalysts (Fe/AC and $Fe/AC-SO_3H$) in terms of impregnation ($FeSO_4.7H_2O$ for 8hr) and sulfonation (with high concentrated sulfuric acid 98 % for 15hr under N_2) were successfully synthesized and compared. The synthesized catalysts were characterized using: pH of zero point of charge, bulk density, total acid density, FT-IR spectroscopy, iron stability, TGA, reusability and performance comparison test with D-optimal experimental design through varying pH of the solution. The result shows that $Fe/AC-SO_3H$ with maximum acid density, higher iron stability with high reusable capacity. In addition to this, the performance comparison test ensured a maximum phenol removal efficiency and TOC reduction of 8 % and 21.6 % respectively, for $Fe/AC-SO_3H$ catalyst higher than former catalyst. Thus, from synthesized catalysts $Fe/AC-SO_3H$ was selected based on the above characterization and further performance analysis was taken place to search for optimal condition.

The selected $Fe/AC-SO_3H$ catalyst was studied for its activity to catalyze mineralization of phenolic aqueous solution using heterogeneous fenton process. Design-Expert 7.0.0 three-level-three-factor with full factorial was applied for experimental design and statistical analysis using a respective process variables; reaction temperature 30, 60 and 90℃, hydrogen peroxide concentration of 1000, 3500 and 6000 mg/L and 60, 150 and 240 min of reaction time. From the analysis of experimental results the interaction effects were studied and the optimal mineralization reaction process conditions, which will maximize the percentage of TOC reduction, were found to be 57.12 ℃ reaction temperature, 2869.72 mg/L hydrogen peroxide concentration and 119.38 min reaction time which gave 97.94% of TOC reduction. The experimental results were fitted well with the derived response model with the R^2 statistic measure, it is evident that the fit successfully accounted for greater proportion of variance as all the models explained ≈ 98.08 %, 99.8 % and 89.85 % for temperature 30 ℃, 60 ℃and 90 ℃ respectively, of the total variation in the data. In average only 4.09 % of the total variations were not explained by FKM and GLKM. However, as GLKM contains more coefficients than the FKM, R-square statistic, a generally accepted best indicator of the fit quality in the comparison of models with those that are nested, is used.

Keywords: *Sulfonation promoted catalyst; phenol mineralization; iron stability; catalyst reusability*

ACKNOWLEDGMENT

First of all I would like to thank the Almighty GOD for giving me the strength and wisdom to successfully complete this thesis. Moreover, I would like to express my genuine appreciation and thank to my Instructor and now this thesis research Supervisor Dr. Beteley Tekola, for his appreciable guidance, diligent advising, for sharing his knowledge, skill, experience and fine-tuning starting from the development of proposal up to the successful completion of this thesis.

I would like also to express my gratitude to the laboratory technicians of the chemical engineering department to Mrs. Hintsasilase Sefu, Mr. Aklilu, Mss. Fikirte, and Mr. Samson for their time and help during my experimental work; Addis Ababa environmental protection authority staffs especially Ato Kedir, for their professional support to carry out experimental works; and Addis Ababa University science faculty department of chemistry, for their technical cooperation during experimental work.

My deepest gratefulness also goes to my best friends especially Mr. Tilahun Gisila, Ms. Frehiwot T/Mariam and Mr. Kitaw abriham for being there and helpful in many ways.

Thanks to my Mom (Zewditu A.) and Dad (Geremew S.) who support throughout this thesis work. I would also like to thank every author, researcher and pioneer whose publications helped me piece this thesis.

TABLE OF CONTENTS

LIST OF TABLES

LIST OF FIGURES

ACRONYMS

AAP	Amino – Antipyrine
AC	Activated Carbon
ANOVA	Analysis of variance
AOP	Advanced Oxidation Process
ASTM	American Section of the International Testing Materials
BD	Balk Density
BOD	Biological Oxygen Demand
CBISC	Carbon Based Iron Impregnated and Sulfonation Promoted Catalyst
COD	Chemical Oxygen Demand
EC	Emerging Contaminants
EDC	Endocrine Disrupting Compounds
Fe/AC	Iron Impregnated Activated Carbon
Fe/AC-SO3-H	Iron Impregnated and Sulfonated Activated Carbon
FKM	First Order Kinetic Model
FTIR	Fourier Transform of the Infrared Radiation
GLKM	Generalized Lumped Kinetic Model
MSH-D	Digital Magnetic Stirrer with Hotplate
MTBE	Methyl Tertiary Butyl Ether
NOM	Natural Occurring Organic Material
PAC	Powdered Activated Carbon
pHZPC	pH of Zero Point of Charge

RSM	Response Surface Method
TA	Total Acidity
TA	Thermal Analysis
TGA	Thermal Gravitational Analysis
TOC	Total Organic Compound
TPh	Total Phenol
USEPA	United States Environmental Protection Authority
VOC	Volatile Organic Carbon
XRD	X-Ray Diffraction

1. Introduction

1.1. Background

Water is a basic need of life on earth. Although 70% of the earth is water, but only one percent is accessible in form of surface freshwater. This one percent surface water is regularly renewed by precipitation and thus is made available for different activities including metabolism. Nevertheless, Water is the biggest crisis faced by world today. Now day's toxic compounds are released to the surface water from different sources like industries. When these compounds enter the stream, they show adverse effect on water cycle and towards living organisms. Phenol and its compounds are one of the toxic substance (J. Michalowicz & W.Duda, 2007) that present in the wastewaters from many industrial sectors such as dyes, pesticides, plastics, oil refineries, petrochemical plants, coal conversion activities, pharmaceuticals, explosives, herbicides and phenolic resin production. Phenol enters water during the manufacturing and processing steps in these industries.

These compounds are very hazardous due to their poor biodegradability, high toxicity and ecological aspects. The presence of phenol in drinking water and irrigation water represents a serious health hazard to humans, animals, plants and microorganisms. Phenol is a potential carcinogen of human, which raises considerable health concerns, even at low concentrations. Many physical, biological, and chemical processes are used in wastewater treatment. But some contaminants found in wastewater are recalcitrant to some degree to commonly applied processes. Chemical processes arise as remediation systems for industries to fulfill their good conduct sometimes optional, sometimes necessary. Oxidation processes are addressed as viable alternatives when the most common biological treatments are not able to achieve the necessary parameters (ROSSI, 2014). Oxidation processes may mineralize certain compounds and constituents through oxidation and reduction reactions. In comparison with the techniques mentioned above, the employment of new technologies with the generic term "advanced oxidation processes" leads to the decomposition and mineralization of many groups of organic materials.

AOPs have fascinated significant helpfulness in recent years. Depending on the chemical structure of the pollutant molecules, AOPs mineralize numerous pollutants into ultimately non-toxic substances like CO_2 and H_2O and therefore avoid the issue of pollution shifting. The particular importance of these technologies appears to be in destroying biologically non-degradable chemical

structures especially in high concentration such as organic pesticides and herbicides (Piera E. et al., 2000), aromatic structures (Zhang L., Li P. & Gong Z., 2008), organo-halogens (Ormad P., Cortes S. & Puig A., 1997) and petroleum constituents(Saien J. & Nejati H., 2007) in wastewaters.

The Fenton's process is one among other advanced oxidation processes (AOP), based on the generation of highly reactive hydroxyl radicals, which attack the complex molecules (Fenton, 1984). Advanced Oxidation Process (AOP) with Fenton reagent (Fe^{2+}/H_2O_2) helps to degrade organic compounds presented in polluted water. In the specific case of Fenton's reagent, the radicals are produced by the reaction between Fe (II) ions and hydrogen peroxide. Hydrogen Peroxide is a multipurpose oxidant for many systems. It can be applied with or without catalyst. Different catalysts used varies compounds such as; ferrous sulphate and other normally used are iron salts, Al^{+3}, Cu^{+2} (Perkowski J. et al., 2006). Furthermore, the oxidant (H_2O_2) is an environmental friendly compound which self-decomposition leads to non-toxic products (H_2O and O_2).

In this research wastewater with phenolic compound will be treated using heterogeneous Fenton process by means of activated carbon as a support that used to regenerate iron [II] ion instead of enhancing the formation of iron precipitation. This process will be carried out through adjustment of different factors like pH, hydrogen peroxide concentration, reaction temperature and reaction time. Unlike homogeneous Fenton process which can lead to high iron concentrations in solution (50–80 ppm), clearly above the legal limit imposed by the directives of the European Union (2 ppm) (C. Pulgarin, 1995) heterogeneous fenton process has no iron precipitation since a solid catalyst will used as a support. Two types of carbon based catalyst was prepared such as iron impregnated activated carbon with ($Fe/AC-SO_3H$) and without (Fe/AC) sulfonation advancement. The prepared catalysts were characterized using different parameters such as: pH of zero point of charge, acid density, FT-IR, bulk density, TGA, reusability and iron content. One of the prepared catalyst was selected through the characteristics, removal efficiency of phenol and reusability of the catalysts. The selected catalyst was further used to optimize phenol mineralization heterogeneous fenton oxidation process.

1.2. Statement of the problem

Emerging contaminants in wastewater effluents and drinking water influents have become a cause for concern in terms of potential impact on human health. Phenol is one of the contaminating compounds that are extant in the wastewaters from many industrial sectors such as oil refineries, petrochemical and ceramic plants, coal conversion activities, pharmaceuticals, pesticides, dyes, plastics, explosives and herbicides and phenolic resin production. Phenol enters water during the manufacturing and processing steps in these industries. These compounds are very hazardous due to their poor biodegradability, high toxicity and ecological aspects. It is therefore essential to develop effective treatment techniques for the removal. Several conventional techniques have been used to remove the phenol from water: biological treatment (including wetland technologies), packed bed adsorption, membrane separation, reverse osmosis, etc., but the success of those techniques has never been complete for reasons that range from pollutant shifting to poor removal yields. The conventional biological treatment of the organic compounds contained in industry wastewaters has been widely demonstrated; however, it is now known that recalcitrant compounds may contribute to chronic toxicity in reclaimed environments (ROSSI, 2014).

Recently, AOPs technology are a fascinating process to mineralize toxic organic compounds by avoid pollution shifting issues. From different kinds of AOPs; Fenton process is a very promising technology based on the oxidant power of hydrogen peroxide (H_2O_2) catalyzed by iron to endorse the formation of hydroxyl radical ($^{\cdot}OH$) which promote high mineralization of toxic organic compounds at about mild conditions (C. Dong, 1993). Unlike homogeneous fenton process which can lead to high iron concentrations in solution (50-80 ppm), clearly above the legal limit imposed by the derivatives of European Union (2 ppm) (C. pulgarin, 1995), heterogeneous fenton process has no iron precipitation since a solid catalyst will used as a support. However, a methods used to synthesize the catalyst will determine the iron stability and mineralization capacity. According to J. J. Rodriguez, et al., (2009) different activated carbon-supported Fe catalysts have been prepared and tested in CWPO and achieve lower mineralization were obtained in less than 2 h with the best catalyst with weighty iron leachate. The use of appropriate catalysts can substantially decrease the energy consumption of various well known oxidation processes. According to Onda A., et al., (2009), sulfonation of activated carbon enhance the stability and catalytic activity of the catalyst. Thus in this work, two fairly different carbon based catalysts (Fe/AC and $Fe/AC-SO_3H$) in terms

of impregnation with sulfonation advancement have been chosen as catalytic supports to mineralize phenol in aqueous solution.

1.3. Objective of the research

1.3.1. General objective

This research paper studies catalytic phenol oxidation in aqueous solution using Fe – sulfonated carbon based solid catalyst as a support in heterogeneous Fenton process.

1.3.2. Specific objective

The specific objectives are:

- To prepare and characterize two different carbon based catalysts (Fe/AC and Fe/AC-SO3-H) through impregnation and sulfonation mechanism
- To compare the performance (activity (conversion), selectivity (TOC) and stability) of the prepared catalyst and evaluate the effect of sulfonated carbon based solid acid catalyst in Fenton process to mineralize phenol.
- To investigate the main and interaction effect of pH, temperature and hydrogen peroxide concentration on the performance of oxidation of phenol through heterogeneous Fenton mechanism
- To generate model equation and determine the optimal operating condition aiming for maximum percentage TOC reduction
- Determine the effect of mineralization reaction time and analyze the kinetics model on oxidation of phenol through heterogeneous Fenton mechanism

1.2. Significance of the study

One of the most important tasks to maintain our quality of life and guarantee the development of many areas around the world is to preserve the quality of the water resources. The development of techniques that permit the reuse of water, avoiding the pollution by wastewater, becomes progressively more and more important. Therefore this research will have:

- ✓ Greater contribution to effectively eliminate organic compounds in aqueous solution, rather than collecting or transferring pollutants into another phase.
- ✓ Aid in the investigating sustainable and renewable technologies, with the possibility of integrating industry's leftovers with wastewater treatment.
- ✓ Early development of promising systems based on the oxidative power of the Fenton's reagent.
- ✓ Enhance the reuse of water that released from different industries containing phenol.

1.4. Scope of the Study

The thesis work generally covers carbon based iron impregnated and sulfonation promoted catalyst (CBISC) synthesis, characterization, iron stability and reusability. Phenol containing synthetic wastewater was then prepared and heterogeneous fenton oxidation using the synthesized catalysts was performed. Treated wastewater analysis, total phenol removal, mineralization (TOC) and adsorption capacity determination and selection of catalyst was covered by this thesis work. Synthesis and characterization of catalyst, iron loading analysis, preparation of synthetic wastewater, and analysis of wastewater will be done using standard procedures and test methods.

2. Literature review

Organic pollution occurs when large quantities of organic compounds which act as substrates for microorganisms, are released into water courses. The extensive incidence of organic pollutants such as pesticides, pharmaceuticals and personal care products, flame retardants, and endocrine disrupting compounds (EDCs) (J. Routledge & E. Sumpter, 2005) in receiving bodies and drinking water influents has been a global issue of concern for academia and environmental agencies for decades, and more recently in the general public. Trace concentrations of numerous organic compounds including prescription drugs, (emerging contaminants (EC), and biologics, "nutraceuticals," fragrances, sunscreen agents, and numerous others are reported in various wastewater effluents and aquatic systems. In addition to these, increasing levels of naturally occurring organic materials (NOM) directly linked to societal nutrient management practices are of serious consequence for managing water resources (Caliman F. & Gavrilescu, 2009). These compounds and their bioactive metabolites are continually being introduced to the aquatic environment as complex mixtures via a number of routes but primarily through both untreated and inadequately treated sewage. In many cases, these pollutants can be traced back to their incomplete removal and discharge from wastewater treatment facilities. Although the direct effect of these compounds on human health is not yet fully understood the detrimental effect on organisms in these receiving bodies from EDCs has already been demonstrated (J. Routledge & E. Sumpter, 2005), such as the feminization of male fish due to the release of natural hormones (Rodgers-Gray, et al., 2000). Research on organic micro pollutants in relation to the point of wastewater discharge can be divided into two major areas: upstream treatment and downstream monitoring. Developing advanced technologies and improved operation of wastewater treatment plants results in higher quality effluents. At the same time, in the downstream analysis, improved techniques to detect pollutants at lower concentrations and tools to evaluate the toxicity of the contaminated stream, feed back to the upstream process in order to optimize plant operation. With pending water scarcity in many parts of the world, providing clean drinking water and sustainable development will require the use of water recycling in the future and it will be imperative that recycled water will not impact both environmental and human health (Falconer, et al., 2006). Consequently, extensive research and development in both upstream processing and downstream monitoring are needed. Phenol is a class of aromatic compounds which grouped as organic pollutants that are toxic to microorganisms when released to the water bodies and, it is persistence to biodegradation.

2.1. Phenol

Phenol is the common name of hydroxyl benzene (C_6H_5OH) and belongs to the class of organic compounds, commonly referred to as phenols, containing one or more hydroxyl groups attached to an aromatic ring as shown in figure 2.1. In addition to this the generalized physical properties of phenol are shown in table 2.1.

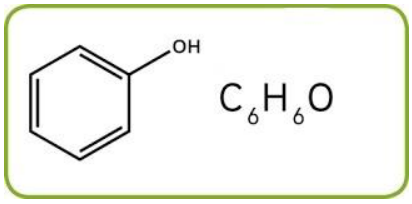

Figure 2.1: Structural formula and molecular formula of phenol

Phenol has also been called carbolic acid, phenolic acid, phenyl hydroxide or oxybenzene. The history of phenol goes back to 1834 when it was first isolated from coal tar and named carbolic acid. Until the advent of synthetic phenol production, just before World War I, coal tar remained the only source of phenol. The first synthetic phenol was produced by sulfonation of benzene and hydrolysis of the sulfonate. More than 99% of phenol produced worldwide is from synthetic processes. In 2001, worldwide phenol production was nearly 6.4 million metric tons (Bizzari, 2002). The predominant uses of phenol are in biphenyl A, Phenolic resins (qv), caprolactam (qv), aniline, and alkyl phenols (qv).

At room temperature phenol is a white, crystalline mass. Phenol gradually turns pink if it contains impurities or is exposed to heat or light. It has a distinctive sweet, tarry odor, and burning taste. Phenol has limited solubility in water between 0 and 65℃. Above 65.3℃ phenol and water are miscible in all proportions.

Although the structure of phenol is similar to cyclohexanol, phenol is a much stronger acid. Its pKa in aqueous solution at 25 ℃ is $9.89 \text{ X } 10^{10}$ (T. Graham, 1992). This characteristic allows aqueous hydroxides to convert phenol into their salts. The salts, especially those of sodium and potassium, are converted back into phenol by aqueous mineral acids or carboxylic acids. Besides being acidic, a significant industrial chemical property of phenol is the extremely high reactivity of its ring toward electrophilic substitution.

Table 2.1: Physical properties of phenol

Property	**Value**
Molecular weight	94.11
Boiling point at 101.3 kPa	181.75
Vapor pressure at 25℃, MPa	46.84
Flash point (closed cup), ℃	79
Density at 20℃ (solid), g/cm^3	1.0722
Critical temperature, ℃	421.1
Critical pressure, MPa	6.13
Specific heat at 14-25 ℃, J/g.K	2.35
Heat of fusion, J/g	121.54
Heat of vaporization, at bp, J/g	528.7
Heat of combustion, kJ/g	-32.468
Viscosity, mPa (=cP)	
At 50 ℃	3.49
70 ℃	2.03
90 ℃	1.26
Specific heat	
At 4.0 ℃ (solid)	1.24
227 ℃ (solid)	1.41
70-74 ℃ (liquid)	2.22

Source: (WALLACE, 2001)

If steric conditions permit, the substitution leads first to the formation of the 2-or 4-mono derivative, then to the 2,4- or 2,6-diderivative, and finally to the 2,4,6 –tri-derivative. The halogenation of phenol produces mono- , di-, and tri-halo phenols.

Phenol and its compounds are present in the wastewaters from many industrial sectors such as oil refineries, petrochemical and ceramic plants, coal conversion activities, pharmaceuticals, pesticides, dyes, plastics, explosives and herbicides and phenolic resin production (Pigatto, et al., 2013). These compounds are very hazardous due to their poor biodegradability, high toxicity and ecological aspects. The presence of phenol in drinking water and irrigation water represents a serious health hazard to humans, animals, plants and microorganisms. Phenol is a potential carcinogen of human, which raises considerable health concerns, even at low concentrations (I.G. Garcia, et al., 1997). Phenol is classified by the USEPA as a priority pollutant. It is therefore essential to develop effective treatment techniques for the removal.

Phenol in a concentration ranging from 50 to 2000 mg per L has been reported by many researchers in industrial wastes Proper treatment of wastewater containing phenol is required before it is discharged to external environment because of its toxicity to living organisms. The permissible limit of phenol is 1 mg per L for industrial effluents to be discharged into inland surface waters (IS: 2490-1974) and 5 mg/L for discharge into public sewers (IS: 3306-1974).

One of the most important tasks to maintain our quality of life and guarantee the development of many areas around the world is to preserve the quality of the water resources. The development of techniques that permit the reuse of water, avoiding the pollution by wastewater, becomes progressively more and more important. Between others, catalysis is a powerful tool for such propose and different kinds of processes have been developed, mainly for the oxidation of organic pollutants.

2.2. Environmental pollution degradation by catalysis

Catalysis is a key technology to provide realistic solutions to many environmental issues, but is also an important marketing opportunity. Environmental catalysis has been recently defined as the development of catalysts to either decompose environmentally unacceptable compounds or provide alternative catalytic syntheses of important compounds without the formation of environmentally unacceptable by-products. Problems addressed in regard to these catalytic

cleanup technologies are mobile emission control, NOx removal from stationary sources, sulfur compounds and VOC (volatile organic compound) conversion, liquid and solid waste treatment and greenhouse gas abatement or conversion. Environmental catalysis also encompasses the application of catalysis for new eco-compatible refinery, chemical or non-chemical catalytic processes, catalytic technologies for minimization of waste, and new catalytic routes to valuable products without the formation of undesirable pollutants.

Historically, the interest of researchers working in the area of environmental catalysis was initially focused mainly on NOx control (mobile and stationary sources), and sulfur and VOC abatement. Scientific interest progressively then moved from the cleanup approach to the other cited subjects. However, recently new problems and questions have renewed research activity in the area of catalytic cleanup technologies. Catalytic technologies for treatment of liquid waste, gaseous emissions and solid waste is necessary in the basic waste management applications.

2.2.1. Catalytic water treatment technologies

Treatment of water bodies contaminated by agricultural practices (nitrate and pesticides, in particular), leakage of non-biodegradable compounds like phenol from different industry and underground fuel tanks and pipelines, and accidental spills and leaking of cleaning solvents, degreasers is becoming a major problem worldwide. There are different aspects of water remediation technologies such as: elimination of nitrate and pesticides from water contaminated by agricultural practices, conversion of MTBE in contaminated underground water, advanced catalytic wet oxidation technologies (of both organics and inorganics, such as phenol), catalytic technologies of wastewater treatment by hydro-treating and photo-catalytic wastewater purification (G. Centi, et al., 2002). Hydrogen processes, commonly known as hydro-treating, are the most common processes for removing sulfur and nitrogen impurities. The oil is combined with high purity hydrogen, vaporized, and then passed over a catalyst such as tungsten, nickel, or a mixture of cobalt and molybdenum oxides supported on an alumina base. Operating temperatures are usually between 260 and 425 °C (500 and 800 °F) at pressures of 14 to 70 bars (1.4 to 7 MPa), or 200 to 1,000 psi. Operating conditions are set to facilitate the desired level of sulfur removal without promoting any change to the other properties of the oil.

2.2.1.1. Advanced oxidation technologies

Advanced oxidation processes are one of environmental catalysis technologies that have attracted significant attention in recent years. Depending on the chemical structure of the pollutant molecules, AOPs mineralize numerous pollutants into ultimately harmless substances like CO_2 and H_2O and therefore avoid the issue of pollution shifting. The particular importance of these technologies appears to be in destroying biologically non-degradable chemical structures as well as ozone-resistant substances such as organic pesticides and herbicides (Sanches, Barreto & Pereira, 2010), aromatic structures (Asadi, et al., 2007), organo-halogens and petroleum constituents (Aljuboury, et al., 2017) in wastewaters.

In a general definition, physicochemical procedures which promote in situ generation of free hydroxyl radicals as highly oxidative reagents for the decomposition of pollutants in water or air are described as "advanced oxidation processes". These oxidation processes basically use three different reagents: ozone, hydrogen peroxide and oxygen in many combinations, either combined with each other or applied with UV irradiation and/or various kinds of catalysts homogeneously and heterogeneously (Dewil, et al., 2017). Due to the generation of increased amounts of OH radicals, combination of two or more AOPs usually leads to higher oxidation rates.

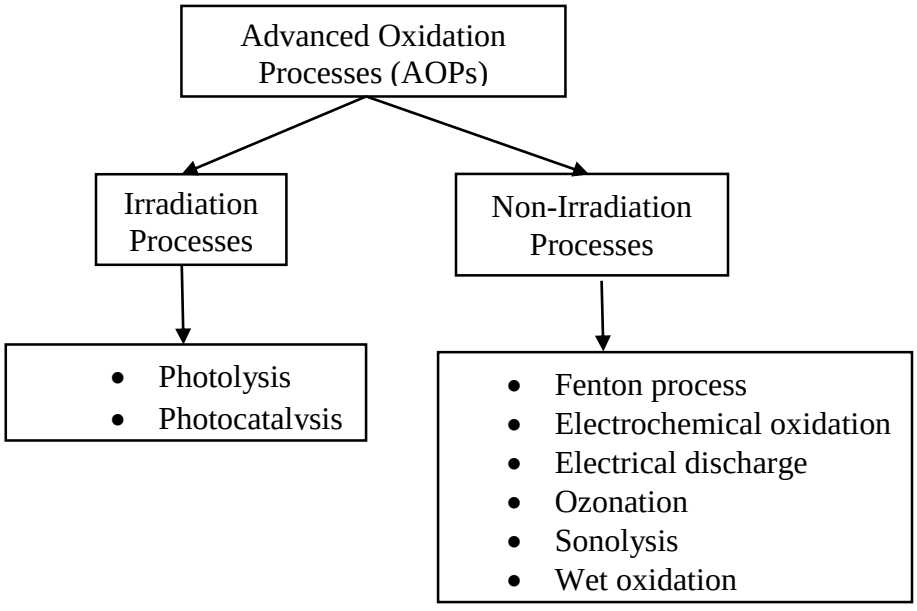

Figure 2.2: Classification of advanced oxidation process

With promising results observed on the laboratory scale, compared with conventional water and wastewater treatment methods, these technologies will likely be more essential for real applications in the near future. However, the reactivity of hydroxyl radicals with radical scavengers (carbonate, phosphate, etc.), which exist in real wastewaters, is the main disadvantage of all oxidative degradation processes based on hydroxyl radical reactions (Kausley, et al., 2017). As shown on figure 2.2, advanced oxidation processes (AOPs) can be classified into irradiation processes (photolysis and photocatalysis) and non-irradiation processes (such as: Fenton process, electrochemical oxidation, electrical discharge, ozonation, sonolysis and wet air oxidation). Some of the most frequently used AOPs are discussed in the following section.

Based on the oxidant power of hydrogen peroxide (H_2O_2) catalyzed by iron ions to endorse the formation of hydroxyl radicals ($\bullet OH$), the Fenton's process (Fenton, 1894) is a very promising Advanced Oxidation Process (AOP) due to the high mineralization promoted at about mild conditions of both temperature and pressure. This treatment technique is, generally, very effective in the depuration of toxic wastewaters (Heponiemi & Lassi, 2010).

2.2.1.1.1. Photocatalytic oxidation

Photo-catalysis is a reaction which uses light to activate a substance which modifies the rate of a chemical reaction without being involved itself. And the photo-catalyst is the substance which can modify the rate of chemical reaction using light irradiation.

This type of advanced oxidation process occurs where a combination of TiO_2, UV light and oxygen is employed for the oxidation and decomposition of an organic compound. Oxygen molecules are adsorbed on UV-illuminated TiO_2 and are involved in a number of reactions.

(Vezzoli, 2012) have reported that the existence of adsorbed oxygen molecules and their reaction with photogenerated electrons on the photocatalyst surface is very important, because it decreases the significance of electron-hole recombination and consequently improves the effectiveness of oxidative paths which include photogenerated holes. Degradation of a large number of chemical substances has been investigated by utilizing the benefits of photocatalytic oxidation(S. boui, et al., 2017).

2.2.1.1.2. Ozonation

Reactions of ozone with organic substances mainly lead to the formation of alcohols, aldehydes and carboxylic acids. Due to the low reaction rate of these oxidation by-products with ozone, very slow further oxidation toward total mineralization by ozone is considered to be the most significant disadvantage of ozonation processes (Nawrocki & Kasprzyk-Hordern, 2010). For this reason, ozonation processes are sometimes considered as pre-treatment oxidation techniques followed by photocatalysis (Sánchez, Peral & Domènech, 1998), or they are modified by adding other elements, introducing a new method known as catalytic ozonation. In the absence of elements, at pH < 3, ozone molecules mainly attack their nucleophilic target organic substance directly, but they gradually and via a chain of reactions decompose to generate hydroxyl radicals and indirectly oxidize substances under conditions of pH > 3. Under these conditions (pH > 3), the existence of hydroxyl radicals accelerates the decomposition of ozone molecules (Nawrocki & Kasprzyk-Hordern, 2010).

2.2.2. Advanced oxidation processes based on iron species

2.2.2.1. Fenton process

A scientist called Henry John Horst man Fenton discovered this process in the end of the 19th century with the oxidation of tartaric acid into di-hydroxymaleic acid by hydrogen peroxide in the presence of ferrous ions (Fenton, 1894). Mechanisms for this reaction were suggested more than thirty years later, in 1932, in two lines: formation of hydroxyl radicals ($\bullet$ OH) followed by autocatalysis (Equations 2.1, 2.2 and 2.3) by Haber and Weiss (1932), while Bray and Gorin (1932) proposed the formation of the ferryl ion (FeO_2^{+}) combined with additional equilibrium to explain the presence of Fe^{3+} (Equations 2.4, 2.5 and 2.6). However, although these two mechanisms are presented in the literature, the one involving hydroxyl radicals is much more accepted and referred.

Haber and Weiss mechanism:

$$Fe^{2+} + H_2O_2 \rightarrow Fe^{3+} + OH^- + OH^* \quad (2.1)$$

$$OH^* + H_2O_2 \rightarrow OH_2^* + H_2O \quad (2.2)$$

$$OH_2^* + H_2O_2 \rightarrow O_2 + OH^* + H_2O \quad (2.3)$$

$Fe^{3+} + H_2O_2 \rightarrow Fe^{2+} + HO_2^{\bullet} + H^+$ ..... (2.4)

Bray and Gorin mechanism:

$Fe^{2+} + H_2O_2 \rightarrow FeO_2^+ + H_2O$ ..... (2.6)

$FeO_2^+ + H_2O_2 \rightarrow Fe^{2+} + H_2O + O_2$ ..... (2.7)

$Fe^{2+} + FeO_2^+ + 2H^+ \rightarrow 2Fe^{3+} + H_2O$ ..... (2.8)

As it is known to all, Fenton process was found more than 100 years ago (Fenton, 1894), and application to destroy the structure of toxic organic compounds was started from late 1960s (C.P. Huang & C. Dong, 1993). It is found that the Fenton reaction could be very efficient in the removal of many hazardous organic pollutants from water and could completely degrade the contaminants to harmless compounds such as CO_2, H_2O and inorganic salts (Neyens & Baeyens, 2003). In recent decades, the mechanism of Fenton process has been widely used in inclusive number of wastewater treatments research such as; homogeneous Fenton and Fenton-like systems using different kinds of Fe (II) and/or Fe (III) salt and peroxide in acidic medium; homogeneous photo-Fenton system by using UV irradiation to reduce Fe (III) to Fe (II); heterogeneous Fenton and Fenton-like system using clay or iron oxides; electro-Fenton or photo-electro-Fenton system.

Among various forms of AOPs, there is a group of typical techniques based on the Fenton reaction, including Fenton, Fenton-like, electro-Fenton and photo-Fenton systems. Fenton mainly based on a series of chain reactions between Fe (II)/Fe (III) species and peroxide (H_2O_2) especially at acidic pH value, which is initiated by the reactions showed in Reaction (Eq.1) and (Eq. 4) (Mora, 2010):

De Laat & Gallard (1999) investigated the mechanism of H_2O_2 catalytic by Fe (III) at acidic pH (pH<3). And at pH 3 to 7, the iron aqua-complex species changed significantly, which accounts for the coagulation capability of Fenton's reagent. Dissolved suspended solids are captured and precipitated (Neyens & Baeyens, 2003), hence the whole Fenton process is retarded to a large extent.

In some researches, UV-irradiation was introduced into Fenton process, which is called as photo-Fenton system. As shown in equation 2.9 and 2.10, the introduction of light, there is also some supplement to the Fenton mechanism (K. Wu, Y. Xie & J. Zhao, 1999).

$Fe^{III}(OH)^{2+} + h\nu \rightarrow \bullet OH + Fe^{2+}$ ..... (2.9)

$H_2O_2 + h\nu \rightarrow 2 \bullet OH$ ..... (2.10)

So far, homogeneous Fenton and photo-Fenton systems have been widely investigated and proved to be efficient in removal of many kinds of organic chemical, especially many non-biodegradable chemicals in aqueous phase, soil and sediment. Furthermore, Fenton process can be used to actual wastewater treatment such as dye wastewater and landfill leachate due to its non-selectivity to organic chemicals (Klauck, et al., 2017). The effect of variables such as temperature, pH value, peroxide concentration and inorganic ions was also determined in these related researches. The advantages and disadvantages of different homogenous Fenton system are concluded and shown in Table 2.2.

Table 2.2: Advantages and disadvantages in different Fenton systems

System	Advantage	Disadvantage
Fenton/Fenton-like	Simplicity: commonly available and inexpensive chemicals, no need for special equipment	Strict pH demand, easy production of iron containing sludge
Photo-Fenton	Lower chemical dosage demand, faster degradation, inexpensive equipment	Strict pH demand, strict wavelength of light usable
Electro-Fenton	Lower chemical dosage demand, faster degradation	Special and quite expensive equipment's demand
Photo-electro-Fenton	Wide application pH value range, Lower chemical dosage demand, high degradation efficiency	Special and quite expensive equipment's demand

When the UV irradiation is introduced into Fenton system, some of the drawbacks could be overcome due to the lower concentration of iron salt needed. (Joseph & J. Pignatello, 1992) compared the degradation of Chlorophenoxy Herbicides in the presence of $Fe\ (III)/H_2O_2$ with

and without UV irradiation respectively, and it has been proved that the presence of UV irradiation could obviously enhance the efficiency of Fenton process in Chlorophenoxy Herbicides degradation, and photo-Fenton is a promising way for wastewater treatment. Some researchers reported the kinetic studies of hydroxyl radical generation promoted by photo-Fenton process ($UV/Fe\ (III)/H_2O_2$) at pH ranging from 3 to 8. And it is found that Fe^{2+}+ reacted with H_2O_2 under UV irradiation could produce •OH radicals at pH ranging from 3 to 8, and proved that such reactions provide a generally important pathway for oxidation in the environment and possibly for the treatment of contaminated waters (Zepp, Faust & Hoigne, 1992). Besides, many studies of organic pollutants treatment based on photo-Fenton process were carried out, and it was practical to apply photo-Fenton system into actual wastewater treatment if the problems such as pH limitation and iron precipitation can be solved.

2.2.2.1.1. Homogenous Fenton process

Homogeneous Fenton's oxidation treatment is an interesting technology entailing simple plants that comprise, generally, a stirred batch tank where pH is controlled within the range 3.0 to 3.5 and operate at ambient conditions of pressure and temperature. $FeSO_4$ Salt is usually applied as Fe (II) source. At the end of the reaction, the effluent is alkalinized and discharged to a tank where the $Fe(OH)_3$ solids, formed by the pH raise, are separated by settling (Bautista et al., 2008). The optimal operational conditions are very dependent upon the type of pollutants to be degraded.

Fenton's reagent efficiency is dependent, amongst other factors, upon pH, hydrogen peroxide, reaction time, temperature and catalyst concentrations. Indeed, pH is a crucial operating parameter. At pH values higher than 4.0, Fe starts to precipitate as iron hydroxide ($Fe(OH)_3$) and H_2O_2 decomposition into oxygen and water is preferred (Szpyrkowicz L.; Juzzolino; C. Kaul, 2001). moreover, the enhancement on the formation of Fe (II) complexes at high pH leads to a drop of Fe (II) concentration (J Benitez et al., 2001). For more acidic conditions, Fe (II) regeneration by the reaction between Fe (III) with hydrogen peroxide is inhibited (J J Pignatello & Huang, 1993). It is, thus, generally accepted that pH 3.0 is the most suitable operating value for this treatment process (Neyens & Baeyens, 2003). The optimum hydrogen peroxide concentration depends upon the specific contaminants; nevertheless, it is generally higher than the stoichiometric quantity theoretically needed to completely remove the effluents of initial TOC since part of H_2O_2

decomposes into water and oxygen via non-radical pathways (Southworth & Voelker, 2003). Even so, the oxidant concentration has to be carefully selected due to its well-known radical scavenger effect. The increase of high ferrous ion concentrations improves the large formation of hydroxyl radicals within a short period of time; nevertheless, Fe (II) itself can be hydroxyl radical scavenger. Generally, Fenton's reaction follows two stages, a first step characterized by a quick degradation (Fe^{2+}/H_2O_2) followed by a slower one (Fe^{3+}/H_2O_2) (Ramirez, Costa & M. Madeira, 2005).

Homogeneous Fenton's process has shown interesting results when applied before biological treatments contributing for the effluents toxicity reduction and biodegradability enhancement (El-Gohary, et al., 2008). Also, the addition of this subsequent step of chemical oxidation can be useful to refine the stream obtained after bio-processing in order to fulfill the regulatory restrictions regarding disposal (Kotsou, et al., 2004). Some of the most important Fenton's characteristics are the low energy requirements (satisfactory results may occur at mild conditions) and the fact that hydroxyl radicals can attack and oxidize organic and inorganic species without specificity due to their very high oxidative power. These radicals are very strong oxidants, with an oxidation potential of 2.8 V – 55 % higher than H_2O_2, its precursor (Kotsou et al., 2004).

The weightiest drawback of homogeneous Fenton's process is the quantity of iron required for the reaction, which is well above the legal amount allowed to effluent discharge. Thus, it becomes necessary to precipitate the iron at the end of the process, which produces a large sum of sludge – a serious environmental problem (Hsueh, et al., 2005). In the sense of avoiding this disadvantage and allowing catalyst recovery, many attempts have been made to use solid catalysts in the Fenton's process. In order to quote a few works dealing with Fe^{2+} regeneration from Fenton's sludge found in the literature, iron-impregnated catalysts have been developed. Qiang, Chang & Huang, (2003) proposed the electro-regeneration which required the solid dissolution by lowering pH to values lesser than 1.0 followed by Fe^{3+} reduction into Fe^{2+} by applying an electrical potential. Meanwhile, different researchers pointed out serious drawbacks to this methodology since the repeated use of the regenerated iron led to effluents with enormously high conductivity due to the extremely low pH needed to re-dissolving the sludge. Besides, it was verified the accumulation of a significant quantity of organic material.

2.2.2.1.2. Heterogeneous Fenton process

The heterogeneous Fenton's process requires a metal-impregnated solid and, in this regard, finding new catalysts and evaluate their efficiency have been the objectives of many studies. Reports have also been published utilizing activated carbons (Pereira, Gonçalves & Órfão, 2014) and soils modified with a catalyst (Dong et al., 2010) combined with ozone as heterogeneous catalysts in recent years. The efficiency of this kind of Fenton process depends mainly on the physical and chemical properties (surface area, porosity, density, pore volume, purity, chemical stability, mechanical strength, presence of active surface sites, etc.) of the surface of the metal oxide and the pH of the solution. As mentioned before, pH is one of the most significant variables in the reaction medium which influences the charge and active sites of the catalyst surface and, consequently, its adsorption capacity as well as the mechanisms of organic compound decomposition in aqueous solutions (Kasprzyk-Hordern, Ziolek & Nawrocki, 2003). Adsorption of organic compounds on the surface of a catalyst is considered to be a key step for heterogeneous catalytic Fenton process. Based on the type of catalyst used in this process, various mechanisms have been described. Zhang, et al., (2008) have suggested that the non-associated catalyst surface hydroxyl groups are active sites for promoting hydroxyl radical generation. There are two major mechanisms have been reported for heterogeneous catalyst. The first is the production of hydroxyl radicals by the adsorption of iron precursor on the catalyst surface and the decomposition of hydrogen peroxide (Cooper & Burch, 1999), and the second is the adsorption and decomposition of ozone/hydrogen peroxide molecules on the surface of the catalyst, leading to the generation of active oxidative surface-bound radicals (Gracia, et al., 2000).

The discovery of ordered porous materials with different topology create different research opportunities across many fields, such as adsorption, separation, and catalysis. Nevertheless, the homogeneous Fenton process can lead to high iron concentrations in solution (50–80 ppm), clearly above the legal limit imposed by the directives of the European Union (2 ppm).

Furthermore, stable Fe^{3+} complexes formed during Fenton's homogeneous processes prevent the Fe^{2+} regeneration (Eq. (2)), affecting the catalytic cycle (Huang, 2013).

In order to avoid these drawbacks related with the homogenous process, iron particles are supported over porous materials. The heterogeneous Fenton's reaction using activated carbons (ACs) as catalysts support has been shown to be a promising process in the wastewater treatment

field, effectively destroying many organics. Moreover, ACs can also remove the pollutant by adsorption or even be catalysts by themselves in heterogeneous Fenton's processes, once the surface of ACs have unpaired π electrons which can react with H_2O_2 leading to hydroxyl radical generation. Actually, activated carbons have shown to be a good choice, being also relatively cheap, with high surface areas and able to be easily modified by suitable treatments (Process, 2015).

Nevertheless, the choice of the appropriate support is not so obvious. Catalyst supports performance in the oxidation reactions depends on the operating conditions employed (temperature, pH, catalyst concentration, etc.), but also on their physical structure (porosity and surface area) and surface chemistry (Rey, et al., 2009). These parameters also determine the chemical nature and dispersion of the metal particles when used as supported catalysts, which defines the final catalytic performance.

The presence of mesoporosity permits a high metal dispersion and consequently a high catalytic activity, however, these catalysts also present the higher leaching degree and thus the optimization of these parameters is a real challenge. In previous works it was found that carbon aerogels are interesting materials for these applications, particularly when iron is the transition metal used as catalyst (Qu & Frias, 2009) and are more promising than activated carbons prepared from agricultural by-products.

2.3. Factors affecting mineralization reaction in heterogeneous fenton process

It's generally known that performance of activated carbon supported heterogeneous fenton process using hydrogen peroxide decomposition to generate hydroxyl radical for phenol mineralization mainly depends on the operating condition employed such as; temperature, pH, peroxide concentration and reaction time.

2.3.1. Hydrogen peroxide concentration and Reaction Temperature

Hydrogen peroxide concentration plays a crucial role in deciding the overall efficiency of the Fenton degradation process. Increasing dosage of hydrogen peroxide will increase the TOC degradation rate of the pollutant (Sivagami, Sakthivel & Nambi, 2017). The unused portion of hydrogen peroxide during the Fenton process contributes to TOC and hence excess amount was not recommended. Another negative effect of excess hydrogen peroxide was the scavenging of

generated hydroxyl radicals (Kausley, et al., 2017). Thus, the dosage of hydrogen peroxide should be adjusted in such a way that the entire amount was utilized and repeatability studies has to be conducted for finding the optimum dosage.

Temperature is one of the important factor influencing catalytic oxidation reaction in fenton. The COD removal efficiency is affected by increasing temperature that increasing the operating temperature has a favorable effect on the organic compound removal (Aygun, 2012).

2.3.2. pH and Reaction time

Fenton process was strongly dependent on the solution pH mainly due to iron and hydrogen peroxide speciation factors. The optimum pH for the Fenton reaction was found to be around 2.8–4 (G. Lofrano, S. Meric & V. Belgiorno, 2007). The activity of Fenton reagent was reduced at higher pH (i.e. > 5) due to the presence of relatively inactive iron precursor and formation of ferric hydroxide precipitate. In this situation, less hydroxyl radicals were generated due to the presence of less free iron ions. The oxidation potential of hydroxyl radicals decreases with increasing pH. At very low pH values, iron complex species [Fe (H_2O)] $^{2+}$ exist, which reacts more slowly with hydrogen peroxide than other species. This phenomenon was also influenced by the concentration of ferrous ion present. In addition, the peroxide gets solvated in the presence of high concentration of H^+ ions to form stable oxonium ion $H_3O_2{}^+$. Oxonium ions make hydrogen peroxide more stable and reduce its reactivity with ferrous (V. Kavitha & K. Palanivelu, 2005). Therefore, the efficiency of the Fenton process to degrade organic compounds was reduced both at high and low pH. At acidic pH of 3–4, Fenton's reagent different effluent was better. Thus an adequate control of pH would increase process efficiency.

Reaction time has also an adverse effect on the efficiency of fenton process. The fenton reaction has a short reaction time among all advanced oxidation processes (Zhang, 2005). According to Long T., et al., (2007) at some optimal reaction time COD decrease gradually and then increase this is interpreted as the reaction between ferrous ion and hydrogen peroxide with the production of hydroxyl radical was almost complete at an optimal reaction time.

2.4. Synthesis of catalyst

2.4.1. Sulfonation of activated carbon

Activated carbon (AC) is widely used as a catalyst support in a variety of industrial and environmental applications for its chemical stability, high specific surface area, and low cost (J. Rodrigues et al., 2017). An early experimental result from Hara's group showed that heating AC in H_2SO_4 only produced a carbon material with a very low SO_3H group density (less than 0.15 mmol·g-1), a fact attributed to the chemical inertness of AC (Hara M. et al., 2004). Onda et al. reported the generation of a sulfonated carbon material with a SO_3H density of 0.44 mmol·g^{-1} by treatment of AC with concentrated H_2SO_4 (Onda A. et al., 2009). The obtained carbon material in this case was quite stable and showed evident catalytic activity for the hydrolysis of cellulose.

According to Masaaki K. et al., (2006) sulfonation of activated carbon is prepared first by drying AC at 378 K in an oven for approximately 8 h. In the sulfonation step, 10 g of the activated porous carbon material was heated in 300 mL of concentrated sulfuric acid (98% conc.) at 353 K under N2 in order to introduce SO_3H. After heating for 10 h and then cooling to room temperature, 1,000 mL of distilled water was added to the mixture, resulting in the formation of a black precipitate, which was then washed repeatedly in boiling distilled water until impurities such as sulfate ions were no longer detected in the wash water. The sample was finally dried overnight in an oven at 373 K to afford the sulfonated acid catalyst.

2.4.2. Impregnation of iron into activated carbon

Recently, activated carbon (AC) has proved to be an excellent catalytic support in the oxidation of aromatic compound (A. Pigamo, et al., 2002) and considerable advance in the understanding of the relationship between the physical and chemical properties of carbon materials and the catalysts efficiency have been carried out in the last few years (A. Quintanilla, et al., 2008).

According to A. Rey, et al., (2009) activated carbon-supported Fe catalysts (Fe/AC) is prepared by incipient impregnation at room temperature from an aqueous solution of different iron precursor, and all samples were left overnight at room temperature, dried during 12 h at 70 ℃, and finally heat treated at 200℃ in air atmosphere for 4 h. According to Plakas & Karabelas, (2016) procedure for preparation iron impregnated powdered activated carbon is shown on table 2.3.

Table 2.4. Preparation procedures of iron-oxide-impregnated PAC adsorbents.

Procedure	PAC/Fe composite	Fe capacity (mg of Fe/g of PAC)	PHPZC
PAC pretreatment			
Fe loading • Addition of PAC (1.0 g) in Erlenmeyer flask containing 100 mL Fe(NO3)39H2O 0.01 M [PAC/Fe(1)] or 0.1 M [PAC/Fe(2)]. • Stirring for 120 min at 200 rpm, 25°C (water cooling system). • Drop wise addition of 1.0 M NaOH until the solution pH reaches 7.0–8.0. • PAC/Fe separation through Millipore 0.45μm and washing with deionized water to remove the salts. • Overnight drying in the oven (~100 °C) and storing of the PAC/Fe adsorbent in a desiccator for further use.	PAC/Fe(1) PAC/Fe(2)	40.7 776.0	7.56 7.80

Source: (Plakas & Karabelas, 2016)

Consequently, two iron loading capacity leads to different PH of zero point of charge which implies different treatment capacity.

PAC pretreatment

- Cleaning of the PAC with absolute ethanol to remove the impurities from its surface and then drying at room temperature for 24 h.

2.5. Analysis of phenol mineralization

The progress of heterogeneous fenton mineralization reaction or the quality of treated waste water, as measured by total phenol concentration using UV-Vis spectrophotometry and TOC reduction used to know percentage of mineralized phenol.

2.5.1. Total phenol content determination

Spectrophotometry is an instrument used extensively for qualitative and quantitative analysis in different fields including environmental control and water management. Spectrophotometric manual 4-AAP is applicable to the analysis of water characteristics. The method is capable of measuring phenolic materials that contain more than 50 $\mu g/L$ in the aqueous phase (without solvent extraction) phenol as standard. It is not possible to use this method to differentiate between different kinds of phenols ("Method 420 . 1" 1978). Phenolic materials react with 4-aminoantpyrine in the presence of potassium ferricyanide at a pH of 10 to form a stable reddish brown antipyrine dye. Method 420 (Appendix C) is used to determine the amount of total phenol in the wastewater.

2.5.2. Total organic carbon (TOC) determination in wastewater

There are a numbers of possible chemical contaminations (compounds), the group of organic compounds is the largest. With an estimated number of more than 19 million, it is impossible to detect and quantify each and every one of them. The sum parameter TOC is one of the most important parameters used in any environmental applications. TOC analysis is therefore carried out in a wide variety of environment matrices: from ground water to seawater, from drinking water to waste water, from soils to sewage sludge.

A total organic carbon analyzer (TOC) measures the carbon content of organic substances in water. One of the most important factor for a TOC analyzer is the ability to oxidize organic carbon. (METH011.00, 2013). The shimadzu total organic carbon analyzer in combination with the ASI-V automated sampler is used to measure TOC in water samples.

2.6. Health effects and Safety Factors

Phenol fumes are irritating to the eyes, nose, and skin. According to the National Institute for Occupational Safety and Health (NIOSH), exposure to phenol should be controlled so that no employees are exposed to phenol concentrations $> 20\ mg/m^3$, which is a time weighted average concentration for up to a 10-hr work day, 40-hr work week. Phenol is very toxic to fish and has a nearly unique property of tainting the taste of fish if present in marine environments at 0.1 – 1.0 ppm (K. Verschueren, 1977). Phenol presents no unusual fire hazard when handled at ambient temperatures, but burns if ignited. The lower flammability limit for the vapor is 1.5 % in air. Phenol produces flammable, toxic vapors at elevated temperatures and has a flash point of 85℃ (open cu p). Phenol is a general protoplasmic poison that is corrosive to any living tissue it contacts. It is a local anaesthetic, so that upon initial contact to the skin no pain is felt. By the time pain is felt, serious burns and absorption through skin may occur. Skin absorption occurs readily with a rapid onset of symptoms or death. Contact with eyes may cause severe damage and blindness. Upon contact with phenol, skin should be washed with water, then washed with poly (ethylene glycol) of molecular weight 300 (Macrogol 300) for at least 30 minutes. Eyes should be washed with flowing water for 10 minutes. Treatment for inhalation begins with removal of the exposed person to fresh air and provision of breathing support if needed (R. J. Lewis, 2004). Personnel who handle phenol should wear protective clothing, safety goggles, and rubber gloves, depending on the working conditions and amount of phenol handled.

3. Materials and Methods

3.1. Materials

The major raw materials used during the experimental work were Activated carbon, sulfuric acid, Iron (II) sulfate, sodium hydroxide, sodium chloride, sodium bicarbonate, hydrochloric acid, nitrogen gas, potassium permanganate, 4-aminoantipyrine, ferric cyanide, hydrogen peroxide, Phenolphthalein powder and other chemical reagent necessary for the analysis. All the above chemicals were analytical reagent grade and bought from different chemical companies in Addis Ababa, Ethiopia.

3.2. Equipment used during experiment

The equipment's used during the experimentations includes different size of beakers, graduated cylinder, digital micro-pipet and volumetric pipet, analytical balance (precision is ± 0.01 mg), different styles of burette stopcocks, spatulas, stirring rods, mechanical and magnetic stirrer, different size volumetric glass flasks, different size of conical and Erlenmeyer flasks, sieve, desiccator used to store samples in a moisture-free environment, oven, Jenway model 3510 digital pH meter, crucibles, thermometer, Aluminum foil, oil bath, water bath, hotplate magnetic stirrer, spectrophotometer (Spectro UVD-3000/3200), cuvettes for spectrophotometer, glass test tubes, plastic bags, vacuum pump, filter paper, funnel, Goggles for eyes protection, protective gloves for hand.

3.3. Methods used during experiment

The experimental work was started in December and end in April a total of six months was spent for the laboratory works. Impregnation of activated carbon, washing and sulfonation of the AC and characterization of the catalyst such as bulk density, PH of zero point charge (PHZPC), adsorption capacity, acid density, activity of the catalyst heterogeneous fenton oxidation reaction was done at School of Chemical and Bio Engineering Laboratory, AAiT. There are other characterization that has been done in different place such as FTIR analysis at faculty of natural science chemistry department, TGA analysis at Leather industry development institute, TOC analysis at Addis Ababa environmental protection authority and iron ion loading at JJ Company.

The overall structure of the experimental work is described on figure 3.1.

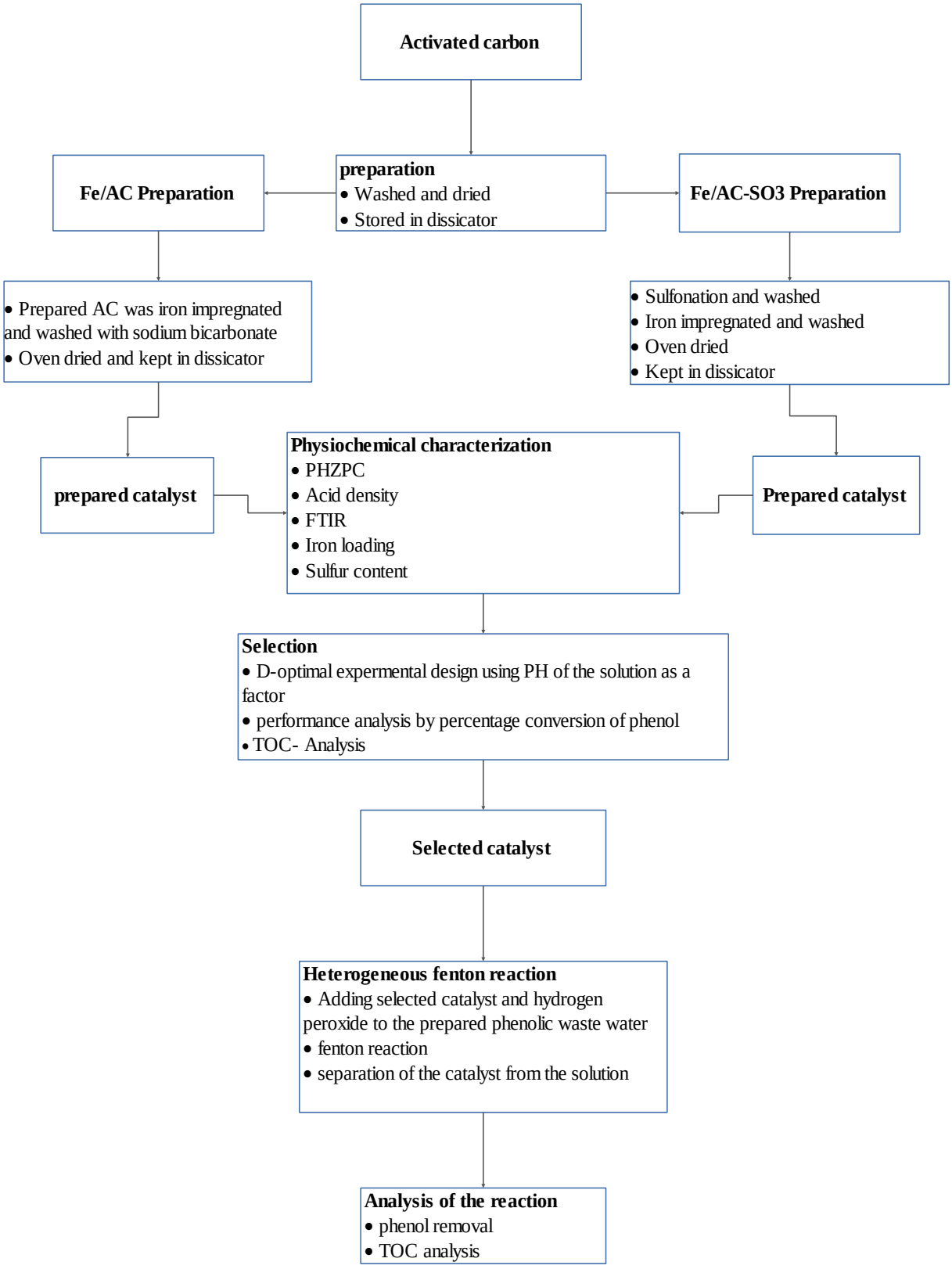

Figure 3.1: Overall structure of the experimental work

3.4. Preparation of Materials and Solutions

3.4.1. Catalyst synthesis

Activated carbon (AC) purchased from Rankem plc. was used for catalyst synthesis by drying in oven. Two catalyst such as iron impregnated activated carbon (Fe/AC) and iron impregnated with sulfonation advancement ($Fe/AC-SO_3H$) was synthesized and used for heterogeneous fenton process. Although the final objective was to optimize the phenol mineralization using the different configurations of carbon supports, this work used to study the performance of the material, and carried out using a batch reactor.

In order to prepare the Fe/AC catalyst wet impregnation method was used. During the impregnation process the activated carbon was rinsed five times in distilled water and dry with 110℃ overnight and cool in a desiccator to avoid moisture absorbance. Impregnation method Shah I., et al., (2015) was used to Coat AC with iron ion, and thermochemical reactions using of 1000 mM $FeSO_4.7H_2O$ solution. Initially, 10g AC was stirred with 1 M $KMnO_4$ solution for 20min at 500 rpm. Afterwards, distilled water was added to dilute the suspension before it was filtered. The residue obtained was then mixed with 1 M $FeSO_4.7H_2O$ and stirred on the magnetic stirrer (MSH-D) up to 8 hr. at the same speed. The suspension was filtered, washed with 1% $NaHCO_3$ and soaked in 1% $NaHCO_3$ solution overnight. Later the suspension was decanted, washed with distilled water and filtered again. In this process, pH of suspension was adjusted to ~8.5 by addition of NaOH and HCl (0.1N) solution. Because the pHZPC of fresh activated carbon is 4.5, increasing the slurry pH to higher than pHZPC leads to negative charge abundance on AC surface and enhancing of impregnation process. The suspension temperature was adjusted on 70°C. Finally, the solid residue was air dried for 2 hr. and then kept in an oven at 110℃ up to 6 hr. for complete drying. The dried sample is the stored in desiccator at room temperature to be used as iron impregnated activated carbon.

For the subsequent catalyst AC was further reacted to attach strong acidic functional groups on the carbon surface based on Nakajima & Hara, (2012) with some modification. In this process 10g of activated porous carbon material is heated in 100ml of concentrated sulfuric acid (98%) at 423 K under N_2 in order to introduce SO_3. After heating for 10h and then cooling to room temperature, 1000ml of distilled water was added to the mixture, resulting in the formation of black precipitate,

then washed repeatedly in boiling distilled water until impurities such as sulfate ions are no longer detected or until pH ≈ 6.5 in the wash water. Finally the sample was dried overnight in an oven at 375K to afford the sulfonated acid catalyst. The sulfonated catalyst is then impregnated with iron sulfate by means of wet impregnation method described above so as to acquire $Fe/AC-SO_3H$ catalyst.

3.5. Characterization of catalyst

The solid structures of Fe/AC and $Fe/AC-SO_3H$ was characterized using pH of zero point of charge, bulk density, iron loading, FT-IR and TGA.

3.5.1. pH of zero point of charge

The pH of zero point of charge (pHZPC) of AC, Fe/AC and $Fe/AC-SO_3H$ was determined following the well-known salt addition method. To a series of Erlenmeyer flask (100ml), 40 ml of 0.1 M $NaNO_3$ solution was added and the pH was adjusted by using HNO_3 and NaOH with variable concentrations (0.1 M) in the pH range of 2-10. To each flask, 0.1g adsorbent was added and the suspensions were agitated at a stirring speed of 200rpm overnight at ambient temperature. The next day, final pH (pH_f) of the suspensions was recorded and the difference between final and initial pH (ΔpH) was plotted against initial pH (pH_i). The pH value where net surface charge was zero, is considered to be the zero point of charge (pHZPC) of the material.

3.5.2. Bulk Density

The bulk density of the AC, Fe/AC and $Fe/AC-SO_3H$ was obtained by weighting a certain grams of the prepared materials and transferring it into a 10 mL graduated cylinder. The cylinder was tamped with a rubber pad while AC and the catalysts was being added until the entire original sample was transferred to the cylinder. Tamping was continued for 5 minutes until there was no further settling produced. The volume was recorded and the bulk density was calculated on the dry basis:

$$\text{Bulk density} = \frac{\text{weight of the sample (g)}}{\text{volume of the sample (ml)}} \quad \text{(3.1)}$$

3.5.1. Determination of the acid density

Acid density of sulfonated carbon was determined by the method reported in the Onda, A. Ochi, & T. Yanagisawa, (2009) with some modification.

The total acid density (-SO_3H, $-COOH$ and $-OH$ groups) of catalyst samples was determined using the standard acid-base back titration method. The catalyst samples were pre-dried in the oven at 105°C for two hours, then 0.05 g of catalyst was added into 20 mL of 0.01N NaOH and sonicated for 1hr at room temperature before back-titration with 0.01N HCl using phenolphthalein as an indicative. Three different acidic groups of sulfonic, carboxylic and phenolic constitute the total acid density.

Calculation for the determination of total acidity (TA):

$$\text{TA} = \text{volume of NaOH} * \text{Normality of NaOH} - \text{Volume of HCL} * \text{Normality of HCL} \quad (3.2)$$

Number of moles of 20 mL 0.01 M NaOH (titrate)

$$0.01 \frac{\text{mol}}{\text{L}} * 20 \text{ mL} * \frac{1 \text{ L}}{1000 \text{ mL}} = 2 * 10^{-4} \text{ mol} \quad (3.3)$$

Number of moles of 0.01 M HCl (titrant) (data obtained from the titrate analysis) is calculated as follows:

$$\text{Number of moles of 0.01M HCl} = \text{Molarity of HCl} * \text{Volume (data from titrant)} \quad (3.4)$$

In a back titration analysis, the acid functional groups on the sample were neutralized with an excessive 20 mL 0.01 M NaOH to ensure a complete neutralization. Therefore, the total acidity of the sample can be calculated as:

$$\text{Total acidity} = \text{mole of 0.01 M NaOH} - \text{mole of 0.01 M HCl} \quad (3.5)$$

$$\text{The total acidity per gram of catalyst } \left(N_{\text{total acidity}}\right) = \frac{\text{total acidity (mole)}}{\text{gram of catalyst used}} \quad (3.6)$$

The sulfonic group density can be determined using the standard base direct titration method. The catalyst was pre-dried in the oven at 105°C for two hours prior to analysis, then 20ml of 0.01N of sodium chloride was added to a 0.05g of catalyst and sonicated for 1hr at room temperature

before direct titrated by 0.01N of sodium hydroxide aqueous solution using phenolphthalein as an indicative. The density of SO_3H group (N mmol/g) was calculated as follows:

$$N_{SO_3H}\left(\frac{mol}{g}\right) = \frac{\text{volume of titrant (NaOH)} * \text{molarity of NaOH}}{\text{mass of carbon}} \quad \text{(3.7)}$$

The density of - SO_3H plus -COOH groups can be determined using the standard acid titration method. The catalyst was pre-dried in the oven at 105°C for two hours prior to analysis. Then, 20ml of 0.01M sodium bicarbonate ($NaHCO_3$) was added to 0.05 g of a catalyst. The solution was sonicated for 1hr at room temperature before acid titrated by 0.01N of HCl aqueous solution using pH meter (until 4 pH). The density of - SO_3H plus -COOH groups (N mmol/g) was calculated as follows:

$$N_{SO_3H,\ -COOH}\left(\frac{mol}{g}\right) = \frac{\text{volume of titrant (HCl)} * \text{molarity of HCl}}{\text{mass of carbon}} \quad \text{(3.8)}$$

Then;

$$N_{OH^-}\left(\frac{mol}{g}\right) = N_{\text{total acidity}} - N_{SO_3H,\ -COOH}\left(\frac{mol}{g}\right) \quad \text{(3.9)}$$

$$N_{-COOH}\left(\frac{mol}{g}\right) = N_{SO_3H,\ -COOH}\left(\frac{mol}{g}\right) - N_{SO_3H}\left(\frac{mol}{g}\right) \quad \text{(3.10)}$$

3.5.2. Fourier Transform of the Infrared Radiation (FTIR)

Fourier-Transformed Infrared (FTIR) spectroscopy is used to analyze relevant characteristics of the prepared catalyst. The analysis can be performed to determine the nature of pollutants, but also to determine the bonding mechanism in case of pollutants removal by sorption processes. The FTIR spectra were recorded on spectrum 65 FT-IR (Perkin Elmer) equipped with KBr beam splitter. A regular scanning range of 400-4000 cm-1 was used for 20 repeated scans at a spectral resolution of 4 cm-1. All the spectra were recorded and processed using essential FTIR software. Thus analyze the compositional and structure of the prepared catalyst using FTIR, first the sample was shaped as a pellet and encumbered in the fitting position. The IR radiation from the source that hits the beam splitter was partly directed towards the two mirrors. One of the two mirrors is stationary, and the other is moved at a constant velocity during data acquisition. Then the IR beams are reflected by mirrors, after that are recombined at the beam splitter, and then passed through the sample and reach the detector. This records all wavelengths in the IR range. After the two beams

reflected by the mirrors recombine, they will travel different distances, and the recombination will lead to constructive and destructive interference. After the recombined beam has passed through the sample the detector will record the Fourier transform of the IR spectrum of the sample. The data obtained were then processed by origin lab software on a computer to draw the graph of percent transmittance versus wavelength.

3.6. Thermal gravimetric analysis

TGA is one of the most important thermal analysis techniques used for the determination of thermal stability of materials. The thermal degradation behavior of the catalyst was investigated through simultaneous plotting of TGA curves. Thermo gravimetric analyzer (TA instrument, model: SDT Q600) was used to determine thermal stability characteristics of $Fe/AC-SO_3H$ catalyst composites using temperature programming from atmospheric temperature to 800℃ at the heating rate of 20℃/min. Testing was carried out under inert atmosphere (N_2) with a flow rate of 2 ml/min to remove all corrosive gases and avoid thermo-oxidative degradation. The thermal degradation onset temperature and the thermal degradation weight loss of composites were recorded and analyzed.

3.7. Performance analysis of the catalysts

3.7.1. Analysis for Phenol adsorption

Prior to phenol oxidation runs, phenol adsorption tests were carried out in order of discriminating adsorption from fenton oxidation reaction. The adsorption test was taken place by adding the activated carbon and the catalysts (without hydrogen peroxide addition) through shaking for about 4 hour. The adsorbed TOC (%) after 4 h contact time was then tested using TOC analyzer. Total organic carbon (TOC) was measured using a TOC analyzer with infrared detector TOC-Vsch., Shimadzu.

3.7.2. Comparing mineralization capacity of the catalysts

In this study, the experimental optimization of phenol removal through fenton process in presence of two heterogeneous catalyst was investigated. Two synthesized heterogeneous catalysts namely Fe/AC and $Fe/AC-SO_3H$ were taken into account for comparative purpose. Table 3.1 shows the D-optimal experimental plan that was applied to obtain regression models which were

subsequently used for the detection of optimum process conditions (pH) at constant hydrogen peroxide concentration (2500 Mg/L), reaction time (120 min) and reaction temperature (50 ℃).

Table 3.1: D- Optimal experiment for pH optimization and catalyst selection

	Factor 1	Factor 2	Response 1
Std.	A:pH	B:catalyst type	Percentage R. (%)
1	3.00	Fe/AC	
2	3.00	$Fe/AC-SO_3H$	
3	6.00	Fe/AC	
4	6.00	$Fe/AC-SO_3H$	
5	3.75	Fe/AC	
6	3.75	$Fe/AC-SO_3H$	
7	5.25	Fe/AC	
8	5.25	$Fe/AC-SO_3H$	
9	4.50	Fe/AC	
10	4.50	$Fe/AC-SO_3H$	

3.7.3. Investigation of Iron stability of the catalysts

Iron leached to the reaction media was determined by means of o-phenantroline method (Appendix D) using an UV/Vis spectrophotometer at 510 nm with some modification. This analysis will help to identify which type of catalyst leached more. Accordingly, two catalyst Fe/AC and $Fe/AC-SO_3H$ were tested for the stability of the iron.

3.8. Experimental setup

Experimental study was designed to obtain maximum TOC and phenol removal at optimum pH, and the selected experimental parameters as on table 3.2. Phenol (purity over 99%), selected

catalyst, NaOH and H_2SO_4 (for pH adjustment) of analytical grade chemicals used via purchasing from different companies. Synthetic wastewater was prepared with 800 mg/L phenol in distilled water.

Table 3.2: Selected experimental parameters

Parameter	Values	Unit
Time	60, 170 and 240	min
Peroxide concentration	2000,4000 and 6000	Mg/L
Temperature	30, 60 and 90	℃

3.9. Catalytic oxidation of phenol using prepared catalyst

3.9.1. Heterogeneous Fenton Experiment

In the heterogeneous Fenton study, the effects of the peroxide (H_2O_2) concentration, reaction temperature and reaction time was investigated. Fenton experiments was then be performed at initial phenol concentration of 800 mg/L peroxide (H_2O_2) concentrations ranged between 2000 and 6000 mg/L, reaction temperature of 30, 60 and 90℃ and reaction time of 60, 150 and 240 min.

During the experimental studies, the volume of the synthetic wastewater to be taken is 500 ml. Figure 3.2 shows the heterogeneous fenton oxidation experimental procedure taken place in the laboratory. As shown on the figure, heterogeneous fenton experiments was carried out by the addition of $Fe/AC-SO_3H$ and hydrogen peroxide to synthetic wastewater through adjusting pH of the solution, then stir using a MSH-D hotplate magnetic stirrer equipped with a magnetic road for determined temperature and reaction time. At the end of the run, the solution was cooled and poured into the settling tank to separate the settled catalyst from treated waste water.

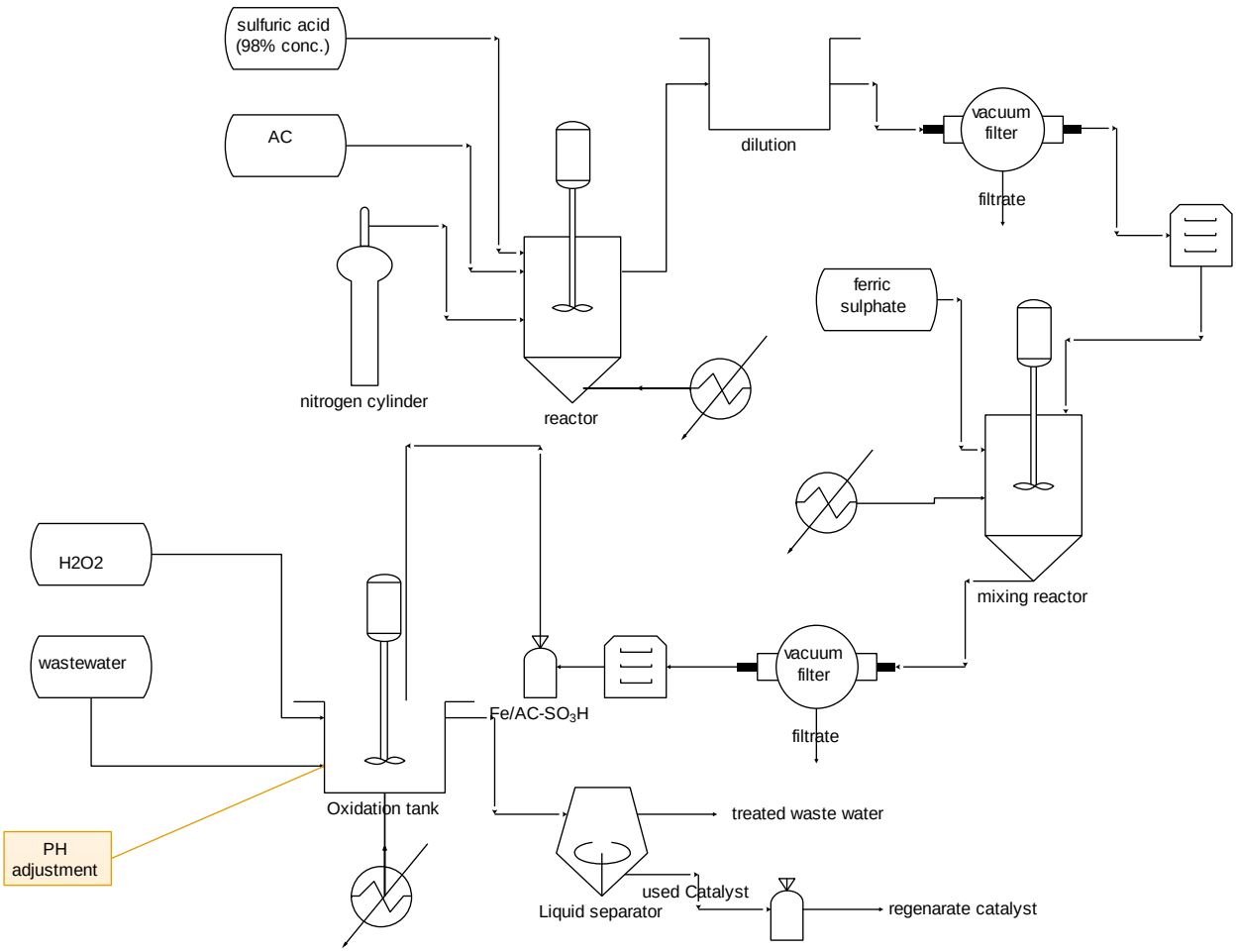

Figure 3.2: Flow diagram of catalyst synthesis and heterogeneous fenton oxidation process

3.10. Performance analysis of Heterogeneous Fenton oxidation

The treated waste water was analyzed for the percentage removal of phenol and mineralization capacity by total organic carbon (TOC) analyzer in order to assess the progress of the treatment over the applied factors. The following topics will illuminate how to identify the above factors during the experimental work.

3.10.1. Total Phenol content

One of the chosen parameters to evaluate the catalysts performances in the Fenton's oxidation was the phenolic content removal. Since the synthetic wastewater solution is exclusively composed by phenol molecule and that was easily broken by the heterogeneous fenton's process, high depletions on this parameter was expected. Also, it was a good way to analyze the initiation of the oxidative

process which was a chain reaction, given that the cleavages generate new radicals that will further react.

After reaction takes place, the total phenol content was determined by Method 420.1 (adapted from ASTM Standard) Phenol (Spectrophotometric, Manual 4-AAP With Distillation) (see appendix-C), (detection limit 0.01 mgL^{-1}). The full spectrum of the standard phenol sample was determined by setting the wavelength 510 nm through diluting the following samples (table 3.3) into 50 mL with volumetric flasks.

Table 3.3: standard preparation for measuring absorbance of phenol

Label	Volume of standard phenol solution (mL)
0	0.00
1	2.00
2	4.00
3	6.00
4	8.00
5	10.00

Absorption of the samples was then measured and the calibration curve with sample 1 to 5 was made in order to determine the concentration of the phenol after treatment with heterogeneous fenton process.

3.10.2. TOC analysis

Total organic carbon (TOC) was measured using a TOC analyzer with infrared detector TOC VSCH. Shimadzu.

3.10.3. Model equation generation using design expert

In this experiment there are three most important factors that will be considered during the experimental work, such as; time, peroxide concentration and temperature with 3 levels. The

response surface method (RSM) was applied to evaluate the effects of reaction parameters and optimize conditions for various responses. Three level factorial design with three numeric factors with five center points was used. Optimal Fenton reaction conditions were determined considering percentage removal of phenol and TOC reduction as response. Treatment of responses and selection of optimal conditions were based on desirability function. The experimental design and multiple linear regression analysis were performed using design expert 7.0.

3.11. Reusability test

The reusability of the Fe/AC and $\mathrm{Fe/AC-SO_3H}$ catalyst was tested repeatedly for four times. After each run, the catalyst was rinsed, dried and used again in the same conditions.

3.12. Mineralization kinetics

The models FKM and GLKM was examined. All Phenol (Ph.) in the wastewater is assumed to be mineralized by only one step in FKM and includes phenol conversion into intermediates in GLKM, where the OH radical generation results in the final products ($CO_2 + H_2O$).

4. Results and discussions

4.1. Characteristics of activated carbon and catalysts

4.1.1. pH of zero point charge

The pH of zero point of charge (pHZPC) corresponds to the pH value at which the surface of the solid is considered to be neutral. It plays an important role during the sorption of ionic species on solid surfaces from aqueous systems. The plots of pHZPC for AC, Fe/AC and $Fe/AC-SO_3H$ are depicted in figure 4.1 below. The result indicate that the surface of Fe/AC and $Fe/AC-SO_3H$ is more acidic with pHZPC of 3.3 and 3.6 respectively. Whereas the surface of AC close to neutrality (pHZPC = 6.5). The lower pHZPC value renders Fe/AC and $Fe/AC-SO_3H$ to be more suitable in the removal of cationic compounds from contaminated wastewater system. The increased acidic character of Fe/AC and $Fe/AC-SO_3H$ reveals that the degree of protonation is inevitably affected by iron impregnation. The modification further contributes to the generation of weak acidic functional groups such as phenolic, lactonic, carbonyl and carboxylic groups on the surface. At the pH values below pHZPC, the Fe/AC and $Fe/AC-SO_3H$ surface is positively charged while at pH above pHZPC the surface of Fe/AC and $Fe/AC-SO_3H$ is negatively charged. At lower pH values (pH 2 and 3) the surface of Fe/AC and $Fe/AC-SO_3H$ undergoes surface protonation due to the frequent interaction and accumulation of H^+ ions from the bulk, which have the tendency to surround the surface of the catalyst. Besides that, the catalysts surface is assumed to release the basic OH^- ions into the bulk which results in a slight increase in the final pH of the suspension. Hence, this results in an overall positively charged catalysts surface at lower pH values (below pHZPC). However, at alkaline pH (or above the pHZPC of Fe/AC and $Fe/AC-SO_3H$), the surface of the catalysts was found to be negatively charged. Generally, with the increase in initial pH of the system, the excessive amount of OH^- ions in the bulk solution are counter balanced by the H^+ ions liberated from the catalysts surface. Moreover, the deprotonation of Fe/AC and $Fe/AC-SO_3H$ results in the decrease in the final pH of the suspension and creates an overall negative charge on the both catalysts surface. The trend in pHZPC values obtained for different catalysts in this work is in close agreement with the reported literature. Previously, Lu et al.,2009 observed a decrease in the pHZPC of oxidized carbon samples modified with nitric acid, 7.72 (AC parent material) to 2.01 for the oxidized AC (v/v ratio of HNO_3 to water, 5:10). The fairly low pHZPC values of these activated carbons were supposed to be due to the oxidation as well as the increase

in acidic surface functional groups on the carbon surface. In another study, the pHZPC values of commercial activated carbon and H_2SO_4 modified carbon black were found to be 6.4 and 3.5, respectively. Herein, the significant decrease in the pHZPC values from 6.5 (AC) to 3.3 and 3.7 for Fe/AC and $Fe/AC-SO_3H$ is attributable to the oxidation as well as the anchoring of iron (Fe) contents on the AC surface upon Fe impregnation.

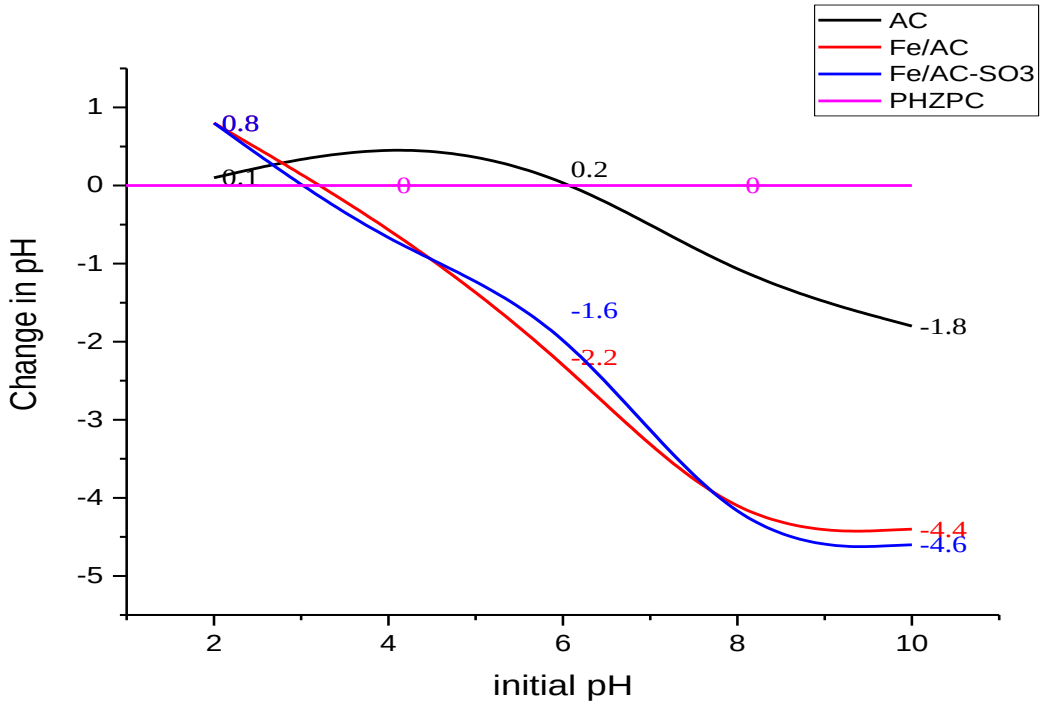

Figure 4.1: Determination of the pH of zero point of charge (pHZPC) for AC and Fe/AC the oxidation followed by the iron impregnation of the carbon surface has changed the PH of the modified carbon.

4.1.2. Bulk density of activated carbon and catalysts

Table 4.1 shows the bulk density of activated carbon as well as the catalysts. The bulk density (BD) of AC, Fe/AC and $Fe/AC-SO_3H$ was determined according to the methods on section 3.4.2 and the detail calculation is attached on appendix A.

As shown on table 4.1 the bulk density of activated carbon is lower than that of catalysts prepared by iron impregnated activated carbon (Fe/AC) and iron impregnated activated carbon with sulfonation advancement ($Fe/AC-SO_3H$).

Hence, sulfonation reaction is sophisticated, many reactions may occur during sulfonation of activated carbon such as complete carbonization and thermal oxidative of the activated carbon.

Table 4.1: Bulk density of AC and the catalysts

Sample	Bulk density (g/ml)	Average bulk density (g/ml)
AC 1	0.3314	0.3492
AC 2	0.338	
AC 3	0.37825	
Fe/AC 1	0.3433	0.4857
Fe/AC 2	0.5247	
Fe/AC 3	0.5893	
$Fe/AC-SO_3H$ 1	0.4472	0.513
$Fe/AC-SO_3H$ 2	0.5075	
$Fe/AC-SO_3H$ 3	0.585	

Since, as long as the bulk density of the activated carbon is lower than that of catalysts sulfonation reaction is the dominant reaction than other possible reactions. However the density of Fe/AC is lower than that of $Fe/AC-SO_3H$ which indicate that some pore volume of the activated carbon is occupied by sulfate ($-SO_3H$) functional group in addition to the iron ion impregnated activated carbon.

4.1.1. Determination of the acid density

Titration method was described in section 3.4.1. Each sample was tested in triplicate. The total acid site density, consisting of carboxylic, phenolic, and sulfonic groups, was measured via back titration method. Table 4.2 shows that the total acid density for both raw activated carbon, sulfonated activated carbon, iron impregnated activated carbon and iron impregnated sulfonated carbon. The detail acid density calculation is described on Appendix-A. The total acid density of

raw activated carbon is lower than that of iron ion impregnated activated carbon, this was expected since wet impregnation method (use of iron sulfate ($FeSO_4.7H_2O$)) enhance to increase the total acidity of the catalyst. Accordingly, the total acid density and density of sulfate group for $AC-SO_3H$ is lower than that of $Fe/AC-SO_3H$ due to the same reason.

Table 4.2: Total acid density

Samples	Total acid density ($mmol/g$)	Density of $-\boldsymbol{SO_3H}$ ($mmol/g$)
AC	0.9	---------
Fe/AC	1.2	---------
AC-SO_3H	4.2	0.62
Fe/AC-SO_3H	5.6	0.74

4.1.2. Fourier Transform Infrared (FT-IR) Spectroscopy

FT-IR analysis results in absorption spectra which provide information about the chemical bonds and molecular structure of a material and also helps to identify the carbon skeleton structure and groups attached on it. The FT-IR spectra for three samples (AC, Fe/AC and $Fe/AC-SO_3H$) were recorded in the range of $4000-400\ cm^{-1}$ and is depicted in figure 4.2.

The band at 3404-3693 cm^{-1} in AC, Fe/AC and $Fe/AC-SO_3H$ spectra can be assigned to the moisture contents which is chemisorbed water in the sample matrix or due to the O-H stretching and bending vibrations as suggested by liu et al., (2009). The absorption bands at 1711-1795 cm^{-1} and 1604 $cm^{-1}$are attributed to COO and $C=C$ stretching vibrations, respectively (Qi et al., 2012). The vibration bands at 1050 cm^{-1} (SO_3^-stretching) and 1495 cm^{-1} (O=S=O stretching in $-SO_3H$) indicate that the as-prepared catalyst materials have surface $-SO_3H$ groups (Suganuma et al., 2008) and are likely to promote solid-acid catalyzed reactions. Therefore, the prepared sulfonated activated carbon materials had an amorphous carbon structure that probably consisted of polycyclic aromatic carbon sheets with randomly attached $-SO_3H$, $COOH$, and phenolic OH groups.

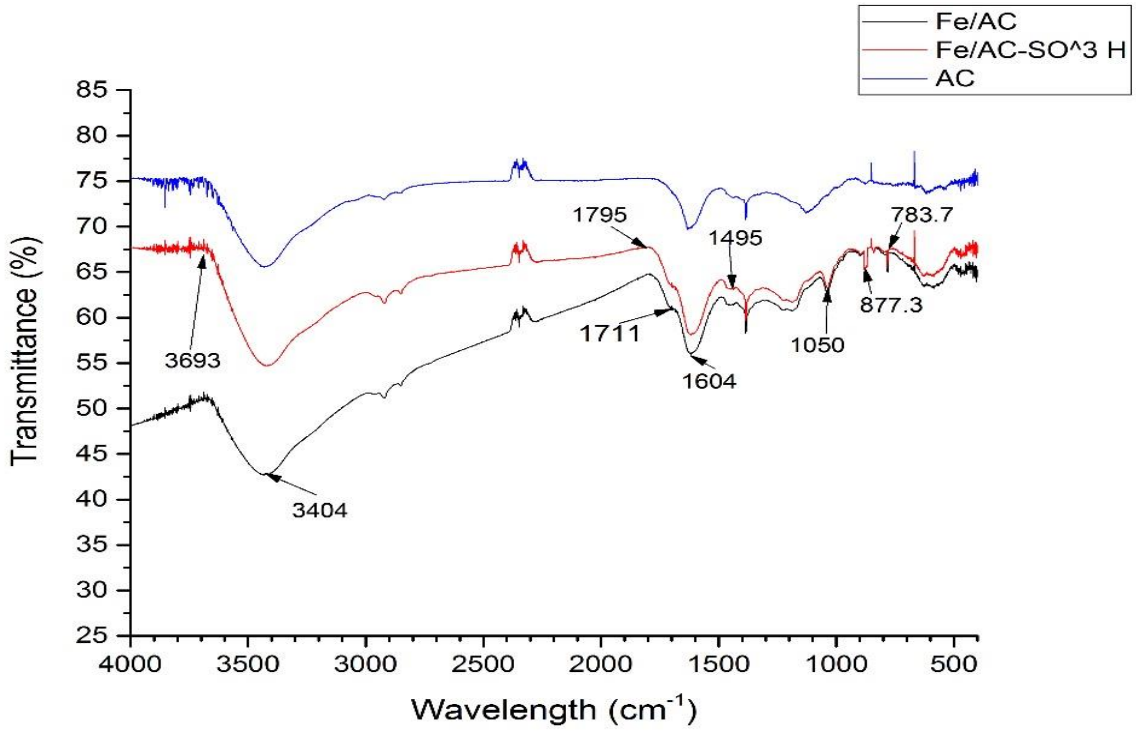

Figure 4.2: FT-IR spectra of activated carbon and synthesized catalysts

Two peaks found at 877.3 and 783.7 cm^{-1} in Fe/AC and $Fe/AC-SO_3H$ can be ascribed by the metal oxygen interactions i.e., $\alpha-FeOOH$ and $Fe-OH$, as described by liu et al., 2009. However, no such peak was found in the FT-IR spectrum of AC. Therefore the catalysts synthesized is clearly iron impregnated and sulphonated according to the data obtained from the FTIR analysis.

4.1.3. Thermo gravimetric Analysis (TGA)

Further investigation on the temperature stability of the catalyst ($Fe/AC-SO_3H$) was performed and the thermal degradation weight loss of composites versus temperature were given in Figure 4.3. As shown in Figure 4.3, the catalyst started to lose weight from 50 °C. This can be attributed to the loss of water absorbed on the surface of the carbonaceous material. The second stage of the weight loss (25% -31%) appeared around 120 ℃ up to 800 ℃ which can be interpreted as due to the decomposition of the $-SO_3H$ groups and Iron (II) ion, and then higher percentage of the catalyst occurred. In addition to the bulk density and acid density TGA also shows the incorporation of sulfonic group to the carbon matrix.

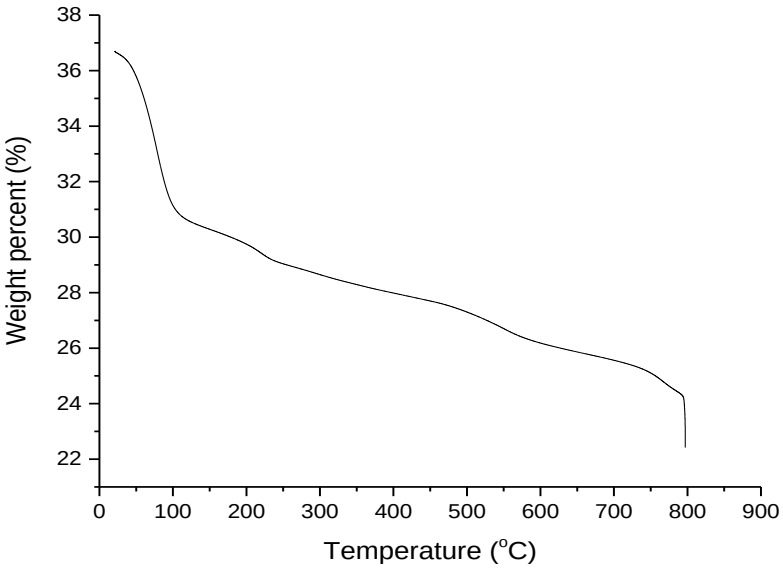

Figure 4.3: Plot of TGA analysis (Weight percent versus temperature)

4.2. Performance test of the catalysts

4.2.1. Performance analysis for Phenol adsorption

Phenol adsorption experiment takes place for AC, Fe/AC and $Fe/AC-SO_3H$ throughout 4 hour contact time with phenol containing wastewater. The degree of phenol removal by both catalyst and activated carbon was calculated as relative to the standard curve equation developed as shown in Appendix-A. The concentration of unknown samples were calculated based on standard curve equation give after absorbance reading. The percentage removal of phenol was then determined using the equation 4.1.

A lower phenol adsorption as can be seen from the values of Tables 4.3 is $Fe/AC-SO_3H$, according with some works in the literature which concluded that phenol adsorption is diminished due to the presence of acid type surface oxygen groups in the AC surface. In addition to this the adsorption capacity of activated carbon is higher than that of the catalysts this is expected since the pore volume of the catalysts become lower because of impregnation and sulfonation processes.

$$\%\ \text{Removal of Ph} = (Ci - C)/Ci * 100\% \quad \text{.....4.1}$$

Where: Ph = phenol

Ci = initial phenol concentration

C = phenol concentration after treatment

Table 4.3: Concentration of phenol adsorbed and percentage removal

Materials	Concentration (with dilution factor=10) (Mg/L)	Average concentration (Mg/L)	Percentage (%)
AC	126.3780108	142.4354397	82.19557004
	170.0164353		
	130.9118731		
Fe/AC	464.7174837	449.9824313	43.75219609
	426.7463871		
	458.4834231		
$Fe/AC-SO_3H$	562.7622556	565.5959195	29.30051006
	550.2941343		
	583.7313687		

4.2.2. Comparing mineralization capacity of the catalysts

Catalyst selection based on the percentage removal efficiency which was measured by 4-AAP method and TOC reduction which is measured by TOC analyzer as described on section 3.10.2. As it can be seen from the figure 4.5 below reveal that phenol was better treated using iron impregnated AC with sulfonation promoted catalyst ($Fe/AC-SO_3H$) at pH of 3.71. Correspondingly higher percentage removal of phenol and TOC reduction with the iron impregnated (Fe/AC) catalysts occurred at pH of 3.71. In addition to this, the difference between total phenol removal and TOC reduction reveals that; at lower pH complete mineralization is favorable than at higher pH. As shown on table 4.4; the solutions for two combination of categorical factor levels such as; Fe/AC and Fe/AC-SO_3H, and three solutions found.

Table 4.4: Solutions for 2 combinations of categoric factor levels and optimum pH

Number	Type of catalyst	PH	Phenol removal	TOC reduction	Desirability	
1	Fe/AC-SO_3H	3.71	99.13	90.8725	0.958	Selected
2	Fe/AC	3.59	91.9692	71.2572	0.703	
3	Fe/AC	3.61	92.0789	70.9937	0.703	

From the solution given by desirability ramp on design expert the later catalyst was selected by desirability of 0.958 at pH of 3.71. Accordingly, further analysis was made on iron leaching of the catalyst to select the optimum heterogeneous catalyst for phenol degradation through heterogeneous fenton process.

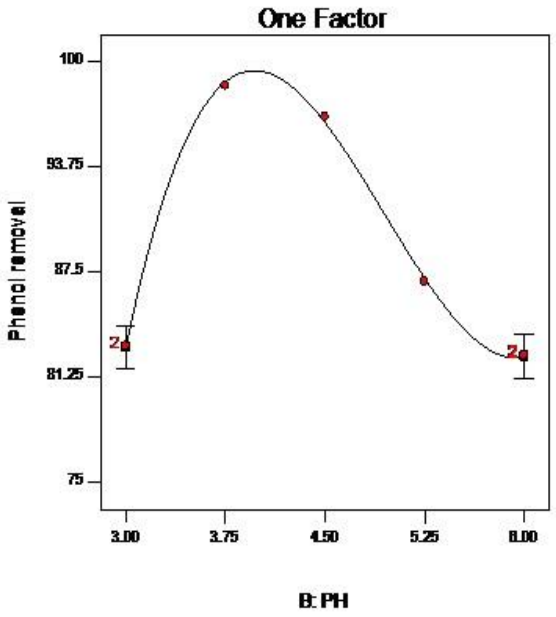

(a)

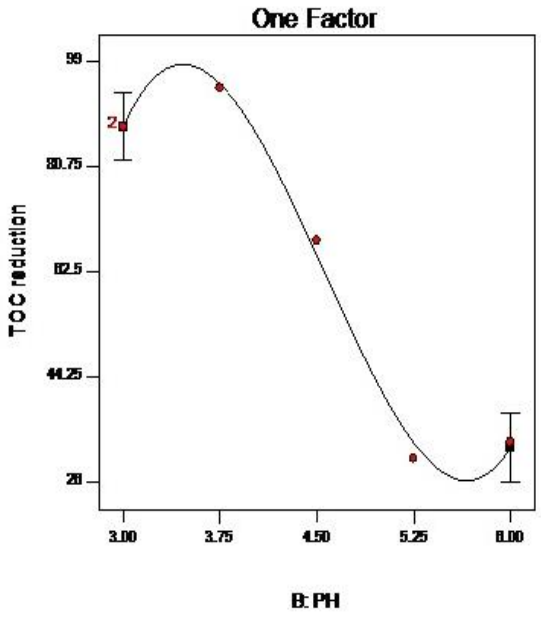

(b)

Figure 4.4: Percentage phenol (a) and TOC (b) reduction versus the pH of the solution

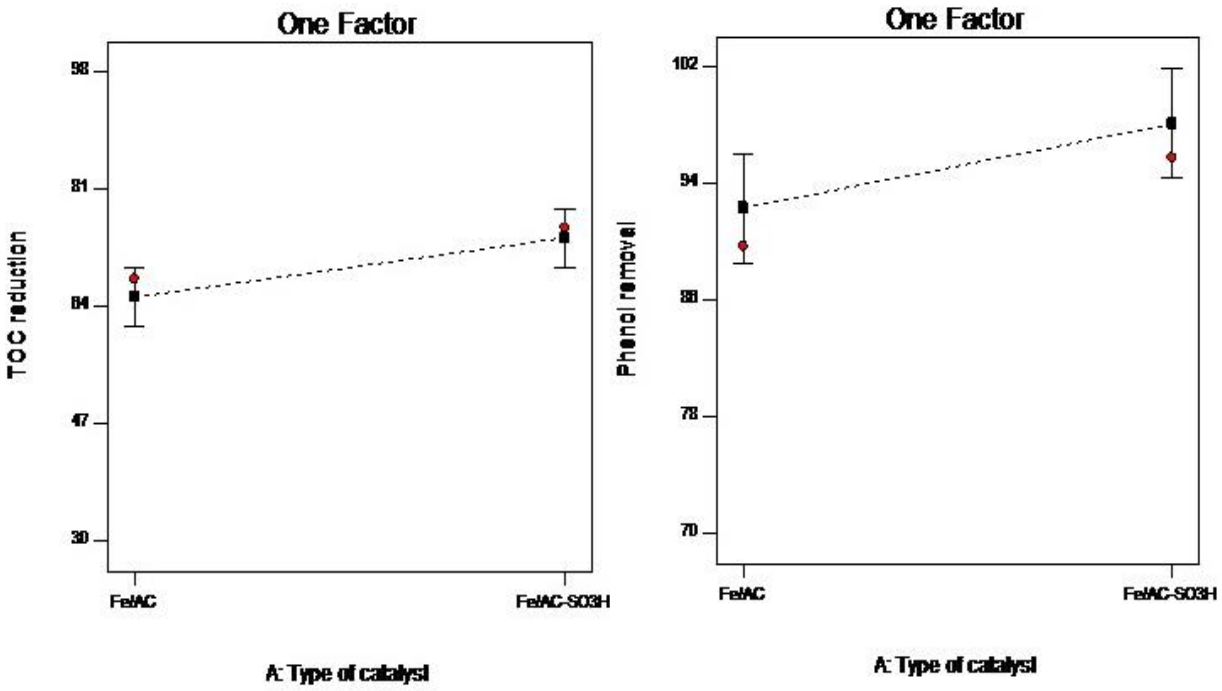

(a) (b)

Figure 4.5: Percentage reduction of phenol (a) and TOC (b) versus type of catalyst

4.2.3. Investigation of Iron stability of the catalysts

Some experiments were carried out to learn on the stability of the iron ion active phase on the catalysts. Figure 4.6 shows the obtained results and the experiments were performed in batch at the conditions described in the experimental section. As can be seen a very fast leaching of Fe takes place in the early stages of contact and after about 40–50 min further leaching becomes almost negligible. The $Fe/AC - SO_3H$ catalyst leads to more stable anchorage of iron than Fe/AC catalyst. The more stable fixation of iron ion is in spite of the fact that as discussed before iron is mainly distributed on the external surface. The higher amounts of oxygen groups of acidic character may be one reason for that. In fact, the highest iron leaching was found for the Fe/AC catalyst which is also the one with a lower amount of acidic (see Table 4.2). The percentage of iron leached from that catalyst reaches close to 20% after 4 h of contact with the oxalic acid solution.

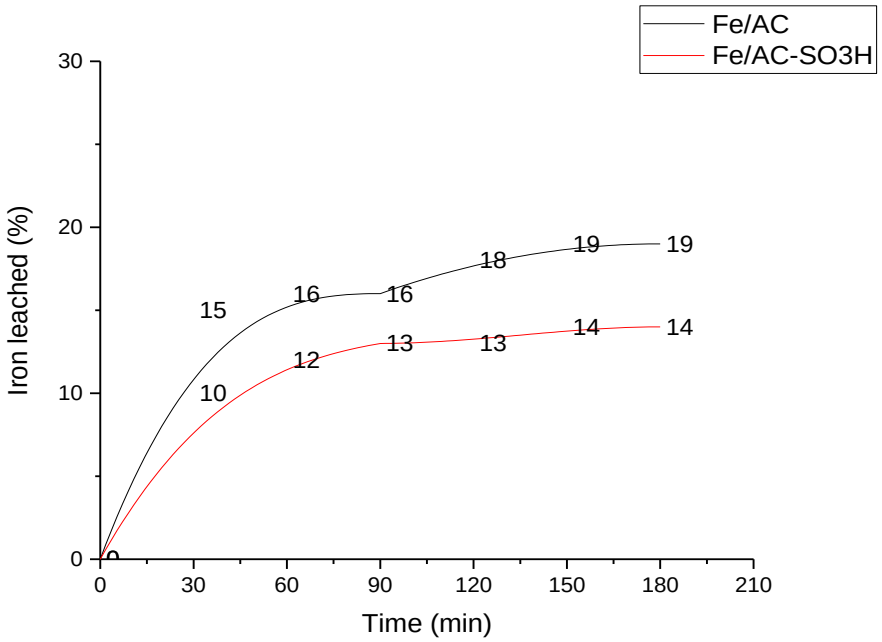

Figure 4.6: Iron leachate versus time of the two catalysts

According to the experiments and tests applied to both proposed catalyst: $Fe/AC-SO_3H$ had a higher peroxide oxidation in heterogeneous fenton process for phenol mineralization as studied in section 4.2.2. In addition to this; the total acidity and amount of sulfate group enhance the stability of the catalyst, $Fe/AC-SO_3H$ had higher iron ion stability than that of Fe/AC catalyst which can contribute for enhancement of reusability. Therefore the catalyst $Fe/AC-SO_3H$ was used for further optimization reaction for heterogeneous fenton oxidation reaction to mineralize phenol.

4.3. Performance analysis for heterogeneous fenton process using $Fe/AC-SO_3H$

Further investigation on the activity the catalyst was performed in heterogeneous fenton process for mineralization of phenol. The heterogeneous fenton reaction was carried out in a batch wise reactor using 750 mL Erlenmeyer flask stirred by magnetic stirrer (MSH-20D) at the following operating conditions: 700 rpm, atmospheric pressure, and 500 mL of reaction volume and an initial pH of 3.7 adjusted using a 0.1N HCl solution and 0.1N NaOH. As described in section 3.8 the optimization reaction was taken place and the performance analysis of phenol mineralization was done using RSM (three level factorial) with five center point and 3 factors, such as temperature (at 30℃, 60℃, and 90℃), peroxide concentration (1000mg/l, 3500mg/l and 6000mg/l) and reaction time (60min, 150min and 240min).

4.3.1. Analysis of model adequacy and response surface methodology

The three-level design or 3k factorial design consider k factors each at 3 level. These are usually referred to as low, intermediate and high levels. The reason that the three-level design were proposed is to model possible curvature in the response function and to handle the case of nominal factors at 3 levels and are purpose built to fit a quadratic model. The RSM (three level factorial) design have runs at the extreme combinations of all the factors with center points of the factor space.

Design-Expert Software 7.0.0 was used in the least squares regression analysis of variance (ANOVA). The statistical software program is used to generate the model equation, interaction effects of the independent variables and surface plots using the fitted equation obtained from the regression analysis holding one of the independent variable constant. The three level full factorial combinations with their respective responses and the ANOVA are given on the table E1 (Appendix E) and Table 4.5 respectively.

The adequacy of the model was further checked with analysis of variance (ANOVA) as shown in Table 4.5, based on a 95% confidence level, F – value is a test for comparing model variance with residual (error) variance. If the variances are close to the same, the ratio will be close to one and it is likely that any of the factors have a significant effect on the response with the P – value less than 0.05. It is calculated by model mean square divided by residual mean square.

The Model F-value 37.69 therefore implies that the model is significant. There is only a 0.01% chance that a "Model F-Value" this large could occur due to noise. Values of "Prob > F" less than 0.0500 indicate model terms are significant. In this case A, B, C, AB, BC, A^2, B^2, C^2 are significant model terms. Values greater than 0.1000 indicate the model terms are not significant.

Lack of fit testing confirmed adequacy of fitting experimental data to a second-order polynomial model, where p-value for lack of fit was insignificant ($p > 0.05$) (Table 4.5). Adequacy of the model was further tested by analysis of variance. The regression model was found to be highly significant with the correlation coefficients of determination of R-Squared, adjusted R-Squared and predicted R-Squared having a value of 0.9391, 0.9142 and 0.8668 respectively. The quality of the model developed could be evaluated from their coefficients of correlation. The value of R-

squared for the developed correlation is 0.9391. It implies that 93.91% of the total variation in the percentage of TOC reduction is attributed to the experimental variables studied.

Table 4.5: Analysis of variance (ANOVA) for the fitted Response Surface Quadratic Model

Source	**Sum of Squares**	**Df**	**Mean Square**	**F Value**	**p-value Prob > F**	
Model	1190.48	9	132.28	37.69	< 0.0001	Significant
A-temperature	*80.75*	*1*	*80.75*	*23.01*	*< 0.0001*	
B-H2O2	*32.21*	*1*	*32.21*	*9.18*	*0.0062*	
C-Time	*43.86*	*1*	*43.86*	*12.50*	*0.0019*	
AB	*20.52*	*1*	*20.52*	*5.85*	*0.0243*	
AC	*0.75*	*1*	*0.75*	*0.21*	*0.6491*	
BC	*19.52*	*1*	*19.52*	*5.56*	*0.0277*	
A^2	*561.18*	*1*	*561.18*	*159.89*	*< 0.0001*	
B^2	*75.82*	*1*	*75.82*	*21.60*	*0.0001*	
C^2	*53.68*	*1*	*53.68*	*15.29*	*0.0007*	
Residual	77.22	22	3.51			
Lack of Fit	*57.80*	*17*	*3.40*	*0.88*	*0.6234*	*not significant*
Pure Error	*19.41*	*5*	*3.88*			
Cor Total	1267.70	31				

A, B, C, representing experimental variables: reaction temperature, reaction time, and hydrogen peroxide concentration respectively.

The quality of the model developed could be evaluated from their coefficients of correlation. The graph of the predicted values obtained using the developed correlation versus actual values is shown in Figure 4.7. The results in Figure 4.7 demonstrated that the regression model equation provided precise description of the experimental data, in which most of the points are close to the line of perfect fit. In addition to this, as shown in figures on (appendix E) diagonistics data plots (normal plot of residuals, residuals vs predicted and residuals vs run) and influence plots (cook's

diatance, DFFITS and DFBETAS) insured there is no any outlayer and the model fits to the expermetal data.

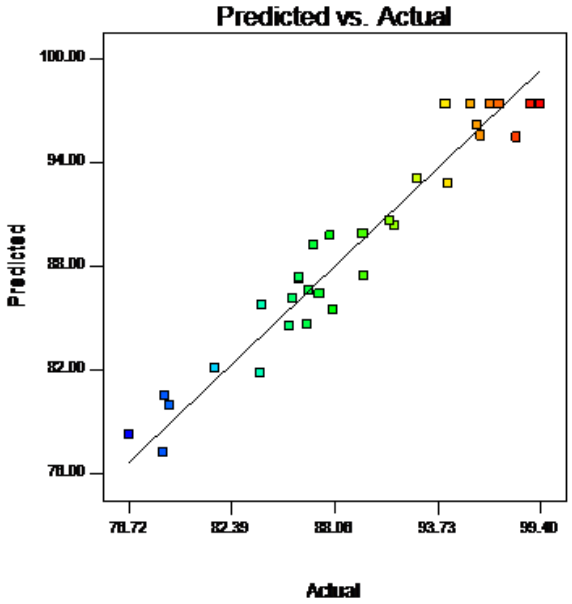

Figure 4.7: Predicted versus actual percentage mineralization of phenol

4.3.2. Effect of process variables on the percentage removal of TOC

The ANOVA of this experimental design shows that, heterogeneous fenton oxidation reaction was significantly affected by various interactions between the process variables. In this study, effects of each process variables and their interaction effects on the target response of phenol degradation was determined. From acquired experimental data and developed model the three dimensional response surface and single factor plots were constructed to illustrate the main and interactive effect of independent variables on the response are shown in Figure 4.8, Figure 4.9 and 4.10.

4.3.2.1. The main effect of Process Variables

The mineralization of phenol catalyzed by the prepared carbon material was examined for different reaction temperatures, hydrogen peroxide concentrations and reaction times. As shown in Figure 4-8 the percentage of phenol degradation is significantly affected by all selected process variables.

It can be seen from the figure 4.8 (a), that with increasing reaction temperature until it reaches about to center value would result increase in the percentage of TOC reduction, the percentage of mineralization then starts to drop as the temperature tend to increase above the center limit. Such behavior could be attributed to the following reasons.

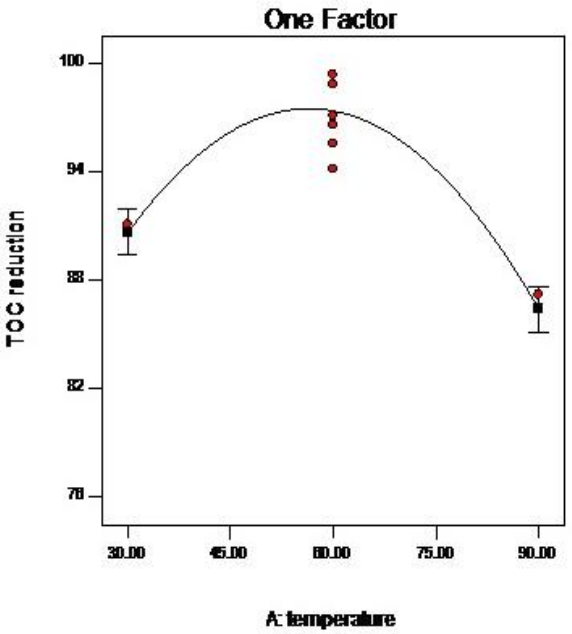

(a)

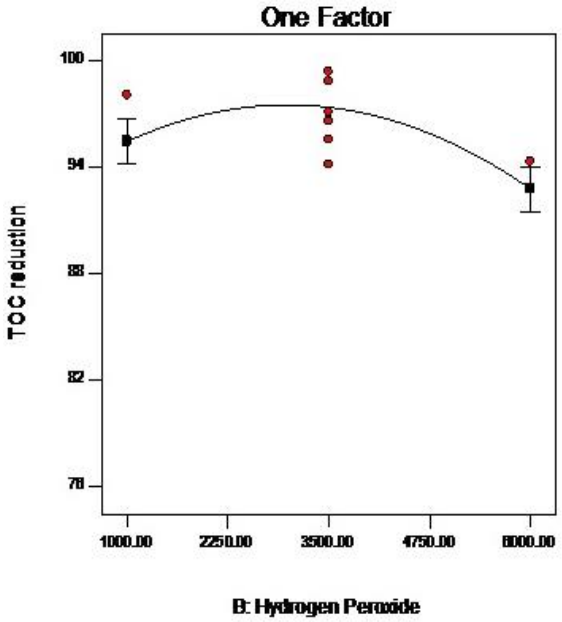

(b)

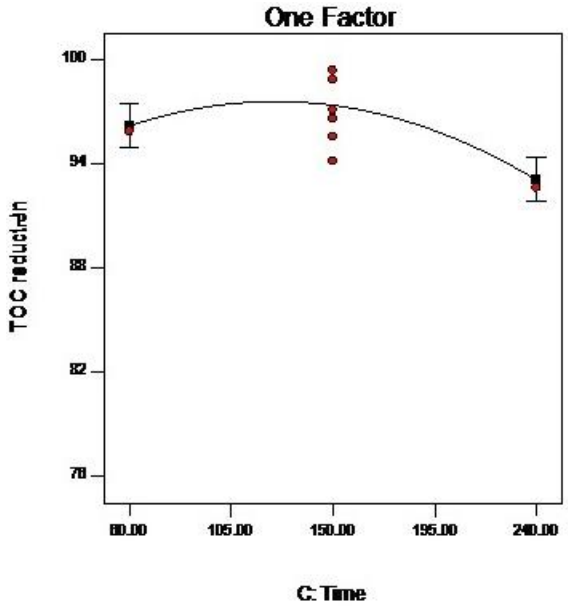

(c)

Figure 4.8: TOC reduction vs. (a) reaction temperature (b) hydrogen peroxide and (c)reaction time

According to ANOVA optimization results suggested that the optimal mineralization level was obtained in a moderate time at lower reaction temperature range (50 to 60℃), at which the mineralization rate was high. According to A. Rey, et al., (2009) also at temperature of 50℃ higher mineralization occurred. In addition to this, figure 4.8 (b) shows that the medium concentration

of hydrogen peroxide enhance the reduction of TOC reduction this can be attributed as effect of excess hydrogen peroxide was the scavenging of generated hydroxyl radicals as stated by Kausley et al., (2017). Which implies that the produced hydroxyl radical is converted to other chemical composition without further mineralizing phenol. Moreover, self-scavenging characteristics of hydroxyl radical as discussed on the literature that the unused portion of hydrogen peroxide during the Fenton process contributes to TOC and hence excess amount was not recommended.

The influence of different reaction times on the TOC reduction is shown in Figure 4.8c. Accordingly, percentage removal of TOC is high at the about medium reaction time interval of 115 to 125 minutes. As described by Comninellis et al., (2008) longer degradation times are required after the removal of the parent compound to achieve complete mineralization in fenton process. In another approach Percentage reduction of TOC decreases as oxidation reaction time increases above a center point, these is expected due the reaction between ferrous ion that are attached to the catalyst and hydrogen peroxide concentration with the production of hydroxyl radical was almost complete after the above specified range of reaction time.

4.3.3. The Interaction Effect of Process Variables for TOC reduction

The most common way to summarize the results of a RSM (three level full factorial) experiment is in the form of three dimensional response surface or contours plot. The process variables were found to have significant interaction effects, the less interaction effect is the interaction of reaction temperature with reaction time and higher interaction is interaction between reaction time with hydrogen peroxide concentration and interaction between reaction temperatures with hydrogen peroxide concentration.

Figure 4.9 and 4.10 shows the interaction effect of reaction temperature with hydrogen peroxide concentration and interaction effect of reaction time with hydrogen peroxide concentration on TOC reduction, respectively. As shown the figure 4.9 (a) the maximum TOC reduction is achieved at lower reaction temperature and medium hydrogen peroxide concentration. From the two interaction effects shown in the figures and contours, at lower range of reaction temperature, hydrogen peroxide at medium range and reaction time at intermediate, always resulted in higher mineralization of phenol than when using lower or higher reaction

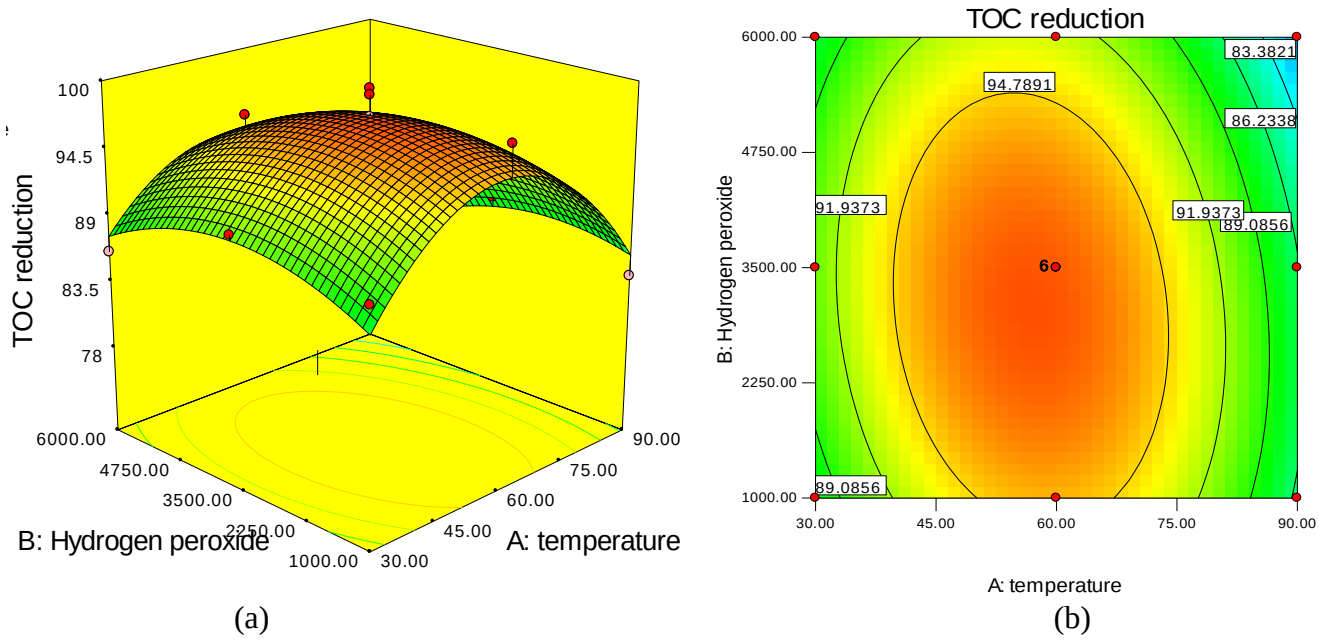

(a) (b)

Figure 4.9: (A) 3D - Surface plot, (B) contour plot of the interaction effect of reaction temperature with amount of hydrogen peroxide versus percentage of TOC reduction when the reaction time is 150 minutes.

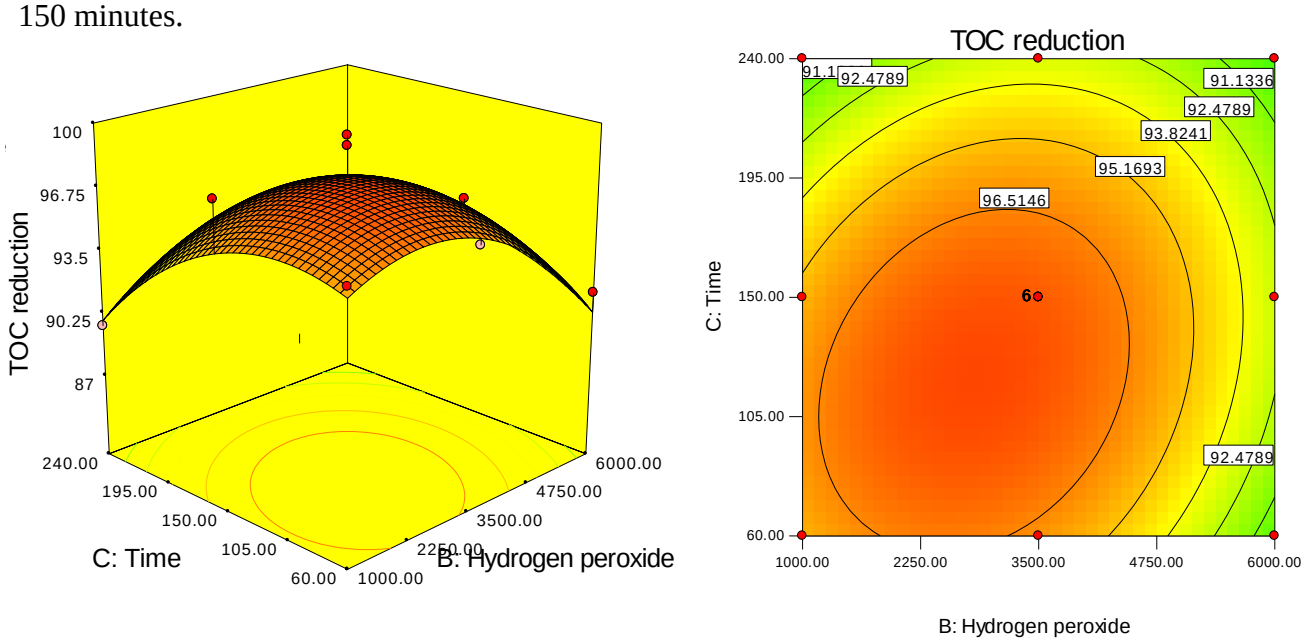

(a) (b)

Figure 4.10: (a) 3D - Surface plot, (b) contour plot of the interaction effect of reaction time with reaction concentration of hydrogen peroxide versus percentage of TOC reduction when the reacion temperature is 60℃.

The above observations can easily be explained as medium hydrogen peroxide concentration, lower reaction temperature and medium reaction time will drive the reaction forward and ensure the mineralization reaction goes to maximum value which results in higher TOC reduction.

Another notable observation is that at higher reaction time, higher amount of hydrogen peroxide concentration and higher reaction temperature is not beneficial in increasing the percentage of mineralization.

This is because at this process conditions, medium reaction time is already sufficient to push the reaction forward. This phenomena is further supported by the fact that both reaction time and reaction temperature is the most significant process variable that affect the percentage of mineralization as indicated by the highest F – value in the ANOVA as shown in Table 4.5.

4.3.4. Development of Regression Model Equation

The model equation that correlates the response (mineralization of phenol) to the Fenton reaction process variables in terms of actual value after excluding the insignificant terms was given below. The predicted model for percentage of TOC reduction in terms of the coded factors is given in equation (4.2).

$$\text{TOC reduction } (\%) = +97.41 - 2.12 * A - 1.34 * B - 1.56 * C - 1.31 * A * B - 0.25 * A * C + 1.28 * B * C - 8.86 * A^2 - 3.26 * B^2 - 2.74 * C^2 \quad \ldots\ldots\ldots\ldots\ldots\ldots\ldots\ldots (4.2)$$

Where:

$A =$ Reaction temperature

$B =$ Hydrogen peroxide concentration

$C =$ Reaction time

4.3.5. Optimization of Process Variables

The results above have shown that the mineralization process variables and the interaction among the variables affect the percentage of TOC reduction. Therefore, the next step is to optimize the process variables in order to obtain the highest percentage of TOC reduction using the model regression developed. Therefore, in order to obtain the maximum percentage of mineralization, the predicted combination of parameters was as follows: temperature of 57.12 ℃, concentration of hydrogen peroxide 2869.72 mg/l and reaction time of 119.38 minutes. Under these conditions, the model predicted TOC reduction of 97.9421% with a desirability value of 0.936.

To validate the optimum conditions predicted by the model using desirability ramp, triplicate experiments were conducted using the optimized mineralization process conditions and mean percentage conversion value of 97.7046% was obtained and the results are closely related with the data obtained from optimization analysis using desirability functions.

Therefore, this study shows that sulfonation can definitely be enhanced for heterogeneous fenton process in mineralizing of phenol and optimum percentage of mineralization can be obtained from the synthesis of iron impregnated with sulfonation advanced carbon catalyst via oxidation reaction.

4.4. Reusability of the catalysts

According to section 3.11 reusability test was taken place and the data and calculation is shown in Appendix A. As shown in Fig. 4.11, the mineralization efficiency of phenol was still high enough, even after four runs. Indeed, the mineralization performance of both $Fe/AC-SO_3H$ and Fe/AC catalysts towards TOC reduction decreased gradually after each run, but it was still higher for $Fe/AC-SO_3H$ catalyst than Fe/AC catalyst after four runs of fenton oxidation reaction. The reasons that may explain the gradual decrease in the mineralization efficiency of phenol would be the iron stability which was higher for the $Fe/AC-SO_3H$ catalyst than that of Fe/AC catalyst contribute to further peroxide oxidation reaction.

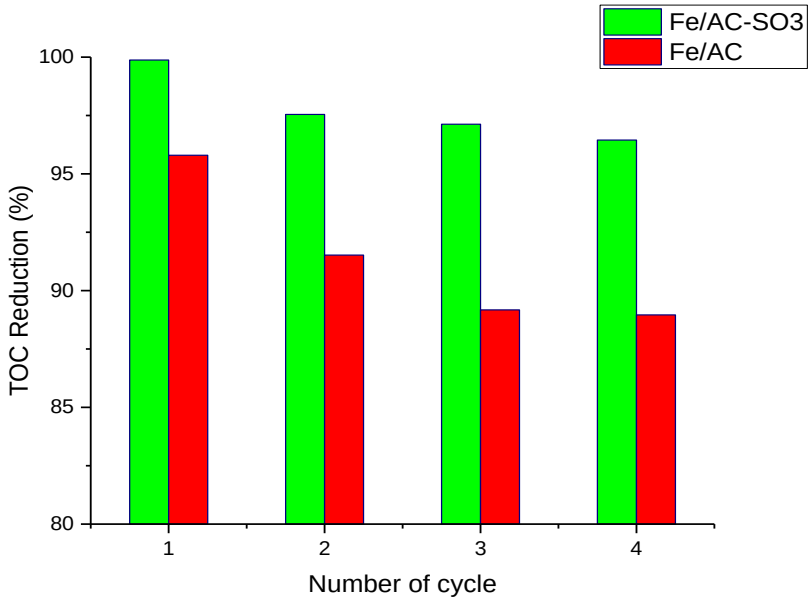

Figure 4.11: reusability graph of percentage TOC reduction versus number of cycles

4.5. Mineralization kinetics

4.5.1. First order kinetic model

The simplest model FKM was examined. All Phenol (Ph.) in the wastewater is assumed to be mineralized in only one step, where the OH addition results in the final products ($CO_2 + H_2O$):

$$\text{Phenol} \xrightarrow{K_3'} CO_2 + H_2O \quad \text{.....} \quad (4.3)$$

Where: - K_3' is the apparent kinetic constant:

$$-r_{TOC_{Ph}} = -\frac{dC_{TOC_{Ph}}}{dt} = K_3' C_{TOC_{Ph}} \quad \text{.....} \quad (4.4)$$

Based on the plot of $-\ln\left(\frac{TOC}{TOC_o}\right)$ against time at different temperature in figure 4.12, the apparent first order kinetic rate constant K_1' and the corresponding correlation coefficients (R^2) of 0.96778 between the experimental and modeled data (Table 4.6), it is observed that the model could well be used to predict the mineralization process.

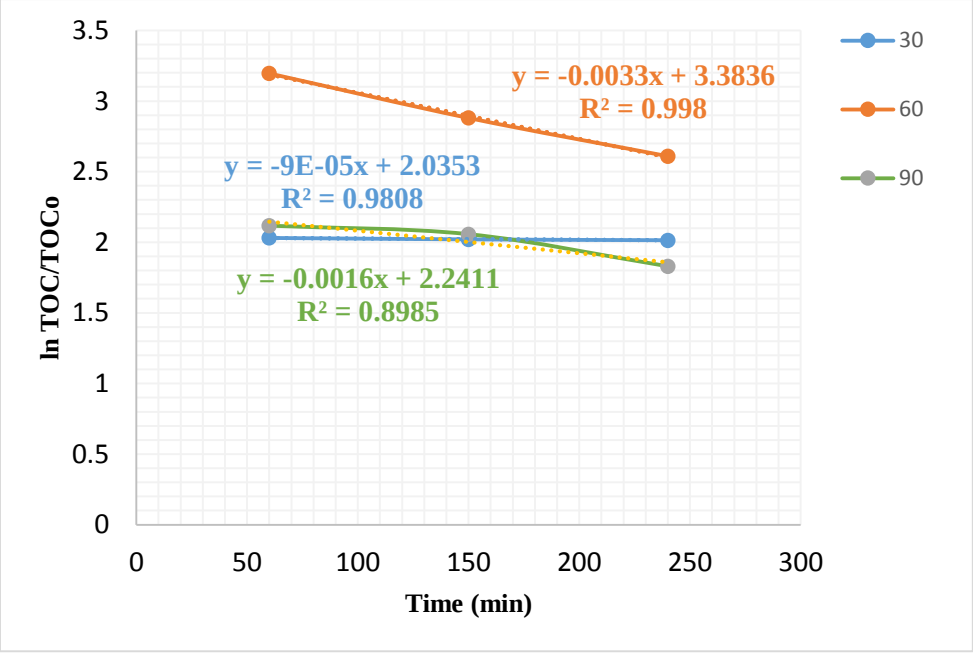

Figure 4.12: plots for FKM and GLKM kinetic model

Data were fitted to the different models, minimizing the sum of squares error (SSE) between empirical and modelled data. Thus, the general assumption that the model will not fit due to the

limitation imposed by the composition of the wastewater appears irrelevant in this case. Although the R^2 and the good agreement the sum of squares error (SSE) suggest explaining the process by the FKM, the limitation imposed calls for further exploring other robust models in addressing kinetic mineralization of such an intricate compound, with a vast diversity of possible reaction pathways.

Furthermore, as the mineralization of phenol is attained in multiple stages involving an initial oxidation step leading to transitional conversion of the contaminants to intermediates and followed by subsequent mineralization of the intermediates to the products, a simple one-step model may not be sufficient. There is need to explore other models.

4.5.2. Generalized Lumped Kinetic Model (GLKM)

Kinetic modeling of solid catalyzed deep oxidation of pollutants in water is crucial to the design and scale-up of wastewater oxidation treatment. Due to their simplicity, the overall kinetics using power-law rates are often unable to capture the important feature in such oxidation systems. However, detailed mechanistic approaches aimed at establishing complex reaction networks where several species and intermediates need to be identified become quickly cumbersome and costly.

A lumped kinetic model that allows insight into the contribution of phenol → intermediates step, which FKM does not account for, is the simple Generalized Lumped Kinetic Model (GLKM). The simplicity of the model relates to its assumption of negligible influence of phenol to $CO_2 + H_2O$ step. To appreciate the need for investigating the intermediates contribution, it's vital to briefly looked at this step. It involves addition of the produced $\cdot OH$ to the wastewater, thereby enhancing the degradability of phenol compound. However, byproducts are generated along time through partial mineralization of the phenol. These intermediates are the results of collapse of aromatic ring during hydroxylation (mineralization), which yields low molecular-weight carboxylic acids (D. Hermosilla & M. Cortijo, 2009).

All of the intermediates that could possibly be produced are lumped into INT, the parent organic substance as phenol (Ph.), while the final mineralization products are $CO_2 + H_2O$. The generalized degradation schemes and kinetic rate constant are shown in Figure 4.13, with $K_1', K_2' and\ K_3'$, , and as the apparent first-order kinetic rate constants for the initial oxidation step, the final oxidation step, and the direct conversion to end products step, respectively.

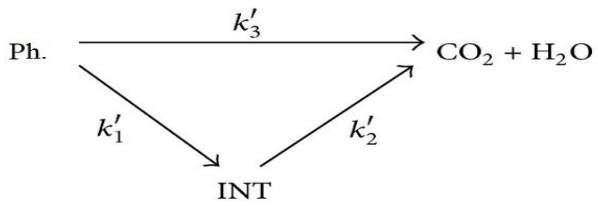

Figure 4.13: schematic representation of phenol mineralization, intermediates, and final product.

Equations (4.5) and (4.6) describe the degradation of phenol and intermediates, respectively:

$$-r_{TOC_{Ph}} = -\frac{dC_{TOC_{Ph}}}{dt} = (K_1' + K_3')C_{TOC_{Ph}} \quad (4.5)$$

$$-r_{TOC_{INT}} = -\frac{dC_{TOC_{INT}}}{dt} = K_2'C_{TOC_{INT}} - K_1'C_{TOC_{Ph}} \quad (4.6)$$

As the mineralization occurs through the transitional conversion to intermediates followed by subsequent mineralization of the intermediates to the products, K_3' is then supposedly to be much smaller than K_1' or K_2' and thus neglected. Hence, by rearranging (4.5) and (4.6), the GLKM becomes

$$\frac{\mathrm{TOC}}{\mathrm{TOC_o}} = \frac{\mathrm{K_1'}}{\mathrm{K_1'+K_3'+K_2'}}\, \mathrm{e}^{-\mathrm{K_2't}} - \frac{\mathrm{K_2'}}{\mathrm{K_1'+K_3'+K_2'}}\, \mathrm{e}^{-(\mathrm{K_1'+K_2'})\mathrm{t}} \quad (4.7)$$

The logarithmic form of (4.7) becomes the following:

$$\ln\frac{\mathrm{TOC}}{\mathrm{TOC_o}} = \ln\frac{\mathrm{K_1'}}{\mathrm{K_2'}} - \ln(\mathrm{K_1'} + \mathrm{K_2'})\mathrm{t} \quad (4.8)$$

The derived Kinetic model equations 4.9, 4.10 and 4.11 for temperatures of 30 ℃, 60 ℃ and 90 ℃ respectively are: the calculations are describe on Appendix A.

$$\ln TOC = 8.37 - \ln t \quad (4.9)$$

$$\ln TOC = 9.72 - \ln(1.0033)t \quad (4.10)$$

$$\ln TOC = 8.58 - \ln(1.0016)t \quad (4.11)$$

From the plot $\ln \mathrm{TOC/TOC_o}$ versus time (Figure 4.12) and the computed rate constant values were marginally different suggesting that the Ph. → intermediates reaction proceeded at the same rate as the intermediates → $\mathrm{CO_2} + \mathrm{H_2O}$ reaction. This result implies that the hydroxylation of the phenol to intermediates cannot be negated.

Table 4.6: FKM and GLKM kinetic rate constants and statistical data

Parameter	FKM			GLKM		
Kinetic rate constant	30 ℃	60 ℃	90 ℃	30 ℃	60 ℃	90 ℃
K_1'	Na	Na	Na	0.88	0.95	0.91
K_2'	Na	Na	Na	0.116	0.0.03	0.0.096
K_3'	0.00397	0.00397	0.00397	Ng	Ng	Ng
Statistical indicators						
R^2	0.9808	0.998	0.8985	0.9808	0.998	0.8985
SSE	0.00418			0.00418		

4.5.3. Goodness-of-Fit Statistics

Two descriptive statistical indicators were used to appraise the prediction performance of proposed models and the produced error in accounting for the kinetic reaction constants and assessing the fit between the experimental data from the models evaluated. The examined indicators were the sum of squares due to error (SSE) and adjusted R-square.

Based on the results summary (Table 4.6), it is seen that there are very small deviations in descriptive performance indices of all the models. GLKM only marginally varied with FKM and demonstrated a slightly superior predictive performance on the estimation of mineralization kinetics. Based on the R^2 statistic measure, it is evident that the fit successfully accounted for greater proportion of variance as all the models explained ≈ 98.08 %, 99.8 % and 89.85 % for temperature 30 ℃, 60 ℃and 90 ℃ respectively, of the total variation in the data. In average only 4.09 % of the total variations were not explained by FKM and GLKM. However, as GLKM contains more coefficients than the FKM, adjusted R-square statistic, a generally accepted best indicator of the fit quality in the comparison of models with those that are nested, is used. Results for SSE show that the total deviation of the response values from the fit-to-the response values measured was acceptable. The lowest values of SSE (0.00418) for GLKM and FKM indicated that

the model performed better. This indicated that the model had a smaller random error component and that the fit would be more useful for prediction.

In summary, the results suggest that both the models adequately describe the kinetics. However, the limitation imposed on FKM does not translate to the real-world description of the process. For instance, mineralization was very fast with respect to the other step, as the kinetic rate constant (K_1') is maximum. This clearly indicates that the initial oxidation step leading to transitional conversion of phenol to intermediates is significantly yet not captured in its entirety in FKM ($0\ \mathrm{min}^{-1}$). In the same vain, rate constant of the intermediates mineralization to the final products preceded fast too (K_2'). Finally, the direct conversion of phenol to end products step (K_3') which was not possible to be captured was found to be appreciable. It is worth noting that mineralization would not have been possible at the rate computed from FKM, especially when steady mineralization was observed within 180 minutes of oxidative treatment period and for fast phenol mineralization.

The use of generalized lumped models becomes necessary in certain reactions. This assertion has been collaborated by several researchers who have elucidated that use of FKM cannot adequately describe the kinetics in systems being continuously fed with H_2O_2 (H. Liu, et al., 2007) , for example, monitoring Fenton oxidation in a semi-continuous reactor where the overall amount of H_2O_2 is distributed as a continuous feed upon the reaction time (W. chu, et al., 2005).

This work provides useful information on complex wastewater treatment by heterogeneous Fenton system, specifically phenol.

5. CONCLUSION AND RECOMMENDATIONS

5.1. CONCLUSION

Phenol compound is very hazardous due to their poor biodegradability, high toxicity and ecological aspects. Oxidation processes may destroy these kind compounds and constituents through oxidation and reduction reactions. The employment of recent technologies with the generic term "advanced oxidation processes" leads to the decomposition and mineralization of many groups of organic materials. Depending on the chemical structure of the pollutant molecules, AOPs mineralize numerous pollutants into ultimately harmless substances like CO_2 and H_2O and therefore avoid the issue of pollution shifting. Based on the oxidant power of hydrogen peroxide (H_2O_2) catalyzed by iron ions to endorse the formation of hydroxyl radicals($\bullet OH$), the Fenton's process is a very promising Advanced Oxidation Process (AOP). In the sense of avoiding ferrous ion precipitation disadvantage and allowing catalyst recovery, use of solid catalysts in the Fenton's process is endorsed. Therefore heterogeneous fenton process which requires supportive material of the catalyst for regeneration is important to overcome this drawbacks. These improvements achieved by having an effective iron impregnated solid acid catalyst that is active in mineralization reactions.

The main objective of this research was to synthesize high surface area, porous, iron stability, and high reusability carbon-based catalysts that have high activities on mineralization reactions. A synthesized catalysts were physically and chemically characterized using pH of Zero Point of Charge (pHZPC), bulk density, acid density, Fourier transform-Infrared spectroscopy (FT-IR), iron leachate, reusability, and further investigation for selected type of catalyst such as thermo-gravimetric analysis (TGA) was performed. Structural study through FT-IR spectroscopy suggests that the catalyst consists of polycyclic aromatic carbon sheets bearing three different acidic groups of phenolic, carboxylic, and sulfonic and the catalyst is stable up to temperature of 120℃. The major contribution was the synthesis of stable and reusable carbon based catalyst using an impregnation and sulfonation method. Activated carbon was used as a catalyst support. Sulfonation of activated carbon in a high concentrated sulfuric acid and iron ion impregnation with magnetic stirring produce two different catalysts. In general, as sulfonation increases the total acid density of the catalyst also increases because total pore volume increased, it was expected that the total acid density of the catalyst samples would increase, as the increase in the pore size would

allow the sulfonic groups to be more easily incorporated onto the carbon matrix. Based on the bulk density, acid density, reusability, iron stability and the performance test using the D-optimal experimental design of the prepared catalysts, catalyst prepared using iron impregnation with sulfonation advancement ($Fe/AC-SO_3H$) was selected for testing the activity of the catalyst.

The mineralization activity of phenol was tested with the major factor that affects the reaction. The reaction parameters affecting the percentage mineralization of phenol were reaction time, reaction temperature and hydrogen peroxide concentration. The outputs of the experiment conducted have been analyzed by employing Design-Expert 7.0.0, surface response methodology, three-level-three- full factor, in which all samples were analyzed by TOC reduction of the treated water. Based on the analysis of experimental results, it is found that all process variables exhibited significant interaction effect on the percentage of TOC reduction. This shows that the capability of the design of experimental analysis in successfully capturing these effects. A reaction temperature of 57.12 ℃, hydrogen peroxide concentration of 2869.72 Mg/L and 119.38 min, reaction time results an optimal value of 97.9421% percentage of TOC reduction which is higher than a similar work done by Rey, et al., (2009) with 85% percentage of TOC reduction catalyzed by Fe/AC.

The experimental results were fitted well with the derived response model with the R^2 statistic measure, it is evident that the fit successfully accounted for greater proportion of variance as all the models explained ≈ 98.08 %, 99.8 % and 89.85 % for temperature 30 ℃, 60 ℃and 90 ℃ respectively, of the total variation in the data. In average only 4.09 % of the total variations were not explained by FKM and GLKM. However, as GLKM contains more coefficients than the FKM, R-square statistic, a generally accepted best indicator of the fit quality in the comparison of models with those that are nested, is used.

In conclusion, activated carbon based catalysts by some means high activity on mineralization reactions were successfully synthesized. The AC-based iron impregnated with sulfonation advancement catalysts are promising catalysts for a more efficient TOC reduction. Nevertheless, investigation on the full life cycle analysis of the carbon-based catalyst preparation ought to be done in order to solve different environmental problems.

5.2. RECOMMENDATIONS

Further investigations are recommended to understand the behavior and to explore their commercial application of the $Fe/AC-SO_3H$ catalysts, such as:

- In this, research the selection of prepared catalyst were performed only based on iron leachate, reusability and D-optimal experimental design with PH optimization of the catalyst but selection of the catalyst based on the surface area, pore size and the activity each catalyst in the reaction by varying different process variables are very important concepts not covered in this research which needs further investigations.
- For more research works on the development of this catalyst, using stronger functionalizing reagents such as fuming acids with higher percentage of free -SO_3H or super acids is recommended.
- Advance investigations on the effect of impregnation of iron and sulfonation process conditions and feedstock on the catalytic activity of AC would be useful.
- Further study on improvement of the mineralization process parameters hydrogen peroxide decomposition, catalyst loading, initial concentration of phenol and speed of agitator on percentage of TOC reduction is also suggested

REFERENCES

A. Quintanilla, N. Mene´ ndez, J. Tornero, J.A. Casas, J. J. R. (2008). physical and chemical properties of carbon material and catalysts. Appl. Catal. B Environ., 81, 105.

Aljuboury, D. A. D. A., Palaniandy, P., B, A. A. H., & Feroz, S. (2017). Treatment of petroleum wastewater by conventional and new technologies - A review, 19(X).

Asadi, M., Shayegan, J., Alaie, E., Faculty, P. E., & Unit, P. (2007). Photocatalytic Degradation of PAHs Contaminated Soil in South Pars Economic and Energy Zone with TiO 2 Nanocatalyst, 4(1), 14–20.

Aygun, A. (2012). effect of temperature on fenton oxidation of young landfill leachate. Global Nest Journal, 43, 142–165.

Bautista, P., Mohedano, A., Casas, J., Zazo, J., & J Rodriguez, J. (2008). An overview of the application of Fenton oxidation to industrial wastewaters treatment. Journal of Chemical Technology and Biotechnology, 83, 1323–1338.

Bizzari, S. (2002). "Phenol,'' Chemical Economics Handbook, SRI Consulting. Menlo Park, Calif.

C. Pulgarin, J. K. (1995). Iron Oxide-Mediated Degradation, Photodegradation, and Biodegradation of Aminophenols, 11, 519–526.

C.P. Huang, C. Dong, Z. T. (1993). Advanced chemical oxidation: its present role and potential future in hazardous waste treatment. Waste Manag.., 13, 361–377.

Caliman F. & Gavrilescu. (2009). Pharmaceuticals, Personal Care Products (PPCP) and Endocrine Disrupting Agents in the Environment. A Review. CLEAN – Soil, Air, Water, 37, 277–303.

Centi, G., Ciambelli, P., Perathoner, S., & Russo, P. (2002). Outlooks for environmental catalysis. Catalysis Today, 75(1–4), 1–2.

Comninellis, C., Kapalka, A., Malato, S., Parsons, S. A., Poulios, I., & Mantzavinos, D. (2008). Advanced oxidation processes for water treatment: advances and trends for R&D. Journal of Chemical Technology and Biotechnology, 83(6), 769–776.

Cooper, C., & Burch, R. (1999). An investigation of catalytic ozonation for the oxidation of

halocarbons in drinking water preparation 1 1 The research was performed in the Catalysis Research Group, Department of Chemistry, University of Reading, Berkshire RG6 6AD, U.K. Water Research - WATER RES, 33, 3695–3700.

D. Hermosilla, M. Cortijo, and C. P. H. (2009). The role of iron on the degradation and mineralization of organic compounds using conventional Fenton and photo-Fenton processes. Chemical Engineering Journal, 155, 637–646.

Dewil, R., Mantzavinos, D., Poulios, I., & Rodrigo, M. A. (2017). New perspectives for Advanced Oxidation Processes. Journal of Environmental Management, 195, 93–99.

Dong, D., Li, P., Li, X., Zhao, Q., Zhang, Y., Jia, C., & Li, P. (2010). Investigation on the photocatalytic degradation of pyrene on soil surfaces using nanometer anatase TiO 2 under UV irradiation, 174, 859–863.

El-Gohary, F., Badawy, M., El-Khateeb, M., & El-Kalliny, A. S. (2008). Integrated Treatment of Olive Mill Wastewater (OMW) by the Combination of Fenton's Reaction and Anaerobic Treatment. Journal of Hazardous Materials, 162, 1536–1541.

Falconer, I. R., Chapman, H. F., Moore, M. R., & Ranmuthugala, G. (2006). Endocrine-disrupting compounds: A review of their challenge to sustainable and safe water supply and water reuse. Environmental Toxicology, 21 (2), 181–191.

Fenton, H. J. H. (1894). Oxidation of Tartaric Acid in Presence of Iron. Journal of the Chemical Society, Vol. 65, 899–910.

G. Lofrano, S. Meric, V. Belgiorno, R. M. A. N. (2007). Fenton's oxidation of various based synthetic tannins (syntans). Desalination and Water Treatment, 211, 10– 21.

Gracia, R., Cortes, S., Sarasa, J., Ormad, M., & Ovelleiro, J. L. (2000). TiO2-catalysed ozonation of raw Ebro river water. Water Research, 34, 1525–1532.

H. Liu, X. Z. Li, Y. J. Leng, C. wang. (2007). "kinetic modeling of electro-fenton reaction in aqueous solution." Water Research, 41(5), 1161–1167.

Hara M, Yoshida T, Takagaki A, Takata T, Kondo JN, D. K., & S, H. (2004). A carbon material as a strong protonic acid. Angew Chem Int Ed 43, 43, 2955–2958.

Heponiemi, A., & Lassi, U. (2010). Advanced Oxidation Processes in Food Industry Wastewater Treatment – A Review, 3(Table 1).

Hsueh, C. L., Huang, Y.-H., Wang, C., & Chen, C.-Y. (2005). Degradation of Azo Dyes Using Low Iron Concentration of Fenton and Fenton-Like System. Chemosphere, 58, 1409–1414.

Huang, W. (2013). Homogeneous and heterogeneous Fenton and photo-Fenton processes : impact of iron complexing agent ethylenediamine-N , N ' -disuccinic acid (EDDS) Wenyu Huang To cite this version : Diplômée de Master Homogeneous and heterogeneous Fenton and photo- Fento 32 (2), 200-277.

I.G. Garcia, J.L.B. Venceslada, P.R. Jimenez Pena, E. R. G. (1997). Biodegradation of Phenol Compounds in Vinasse Using Aspergillus Terreus And Geotrichum Candidum. Water Resource, 31(8), 2005–2011.

J. Michalowicz W.Duda. (2007). Phenols - Source and Toxicity. Polish J. of Environ. Stud., 16, 347–362.

J Benitez, F., Acero, J., Real, F., J Rubio, F., & Leal, A. I. (2001). The Role of Hydroxyl Radicals for the Decomposition of p-Hydroxy Phenylacetic Acid in Aqueous Solutions. Water Research, 35, 1338–1343.

K. Wu, Y. Xie, J. Zhao, H. H. (1999). Photo-Fenton degradation of a dye under visible light irradiation. J. Mol. Catal. A: Chemical, 144, 77–84.

Kasprzyk-Hordern, B., Ziolek, M., & Nawrocki, J. (2003). Catalytic Ozonation and Methods of Enhancing Molecular Ozone Reactions in Water Treatment. Applied Catalysis B Environmental, 46, 639–669.

Kausley, S. B., Desai, K. S., Shrivastava, S., Shah, P. R., Patil, B. R., & Pandit, A. B. (2017). Mineralization of alkyd resin wastewater: Feasibility of different advanced oxidation processes. Journal of Environmental Chemical Engineering, (March), 200, 99-112.

Klauck, C. R., Giacobbo, A., Altenhofen, C. G., Silva, L. B., Meneguzzi, A., Bernardes, A. M., & Rodrigues, M. A. S. (2017). Toxicity elimination of landfill leachate by hybrid processing of advanced oxidation process and adsorption. Environmental Technology and Innovation, 8, 246–255.

Kotsou, M., Kyriacou, A., Lasaridi, K., & Pilidis, G. (2004). Integrated aerobic biological treatment and chemical oxidation with Fenton's reagent for the processing of green table olive wastewater. Process Biochemistry - Process Biochem, 39, 1653–1660.

Long Tengrui, Anas Al-Harbawi, Z. J. and L. M. B. (2007). The Effect and its Influence factors of the Fenton process on the Old Landfill Leachate. Journal of Applied Science, (5), 724–727.

METH011.00. (2013). Water TOC analysis using the shimadzu TOC-VCSN and ASI-Autosampler. California Department of Persticide Regulation, 1–14.

Method 420 . 1 : Phenolics (Spectrophotometric , Manual 4 - AAP With Distillation). (1978).

Mora, E. G. G.-R. and B. K. . T. and M. L. (2010). Clays and oxide minerals as catalysts and nanocatalysts in Fenton-like reactions. Applied Clay Science, 47, 182-192.

Nawrocki, J., & Kasprzyk-Hordern, B. (2010). The Efficiency and Mechanisms of Catalytic Ozonation. Applied Catalysis B-Environmental - APPL CATAL B-ENVIRON, 99, 27–42.

Nejati H., and S. J. (2007). Enhanced photocatalytic degradation of pollutants in petroleum refinery wastewater under mild conditions. Journal of Hazardous Materials, 148, 491–495.

Neyens, E., & Baeyens, J. (2003). A review of classic Fenton's peroxidation as an advanced oxidation technique. J. Hazard. Mater., 98, 33–50.

Onda, A.;Ochi, T.; Yanagisawa, K. (2009). Hydrolysis of cellulose selectively into glucose over sulfonated activated-carbon catalyst under hydrothermal conditions. Catalysis, 52, 801–807.

Ormad P., Cortes S., Puig A., O. J. L. (1997). Degradation of organochloride compounds by O3 and O3/H2O2. Water Research, 31, 2387–2391.

Pereira, M. F. R., Gonçalves, A. G., & Órfão, J. J. M. (2014). Carbon materials as catalysts for the ozonation of organic pollutants in water Materiales de carbón como catalizadores para la ozonización de contaminantes orgánicos en agua, (reaction 1).

Piera E., Caple J.C., Brillas E., Domenech X., P. J. (2000). 2,4-Dichlorophenoxyacetic acid degradation by catalyzed ozonation: TiO2/UVA/O3 and Fe(II)/UVA/O3 systems. Applied Catalysis B: Environmental, 27, 169–177.

Pigamo, M. Besson, B. Blanc, P. Gallezot, A. Blakburn, O. Kozynchenko, S.Tennison, E. Crezzee,

A. F. K. (2002). Catalytic oxidation of aromatic compound. Carbon, 40, 1267.

Pigatto, G., Lodi, A., Finocchio, E., Palma, M.S., Converti, A. (2013). Chitin as Biosorbent for Phenol Removal from Aqueous Solution: Equilibrium, Kinetic And Thermodynamic Studies, 40 (3), 883-967.

Pignatello, J. J. (1992). Dark and photoassisted iron(3+)-catalyzed degradation of chlorophenoxy herbicides by hydrogen peroxide. Environmental Science & Technology, 26(5), 944–951.

Pignatello, J. J., & Huang, L. Q. (1993). Degradation of polychlorinated dibenzo-p-dioxin and dibenzofuran contaminants in 2,4,5-T by photoassisted iron-catalyzed hydrogen peroxide. Water Research, 27, 1731–1736.

Plakas, K. V., & Karabelas, A. J. (2016). A study on heterogeneous fenton regeneration of powdered activated carbon impregnated with iron oxide nanoparticles. Global Nest Journal, 18(2), 259–268.

Process, C. (2015). Novel Hybrid " Powdered Activated Carbon – Fenton Oxidation " Processes for Water Treatment, (September), 3–5.

Qiang, Z., Chang, J.-H., & Huang, C. P. (2003). Electrochemical Regeneration of Fe2+ in Fenton Oxidation Processes. Water Research, 37, 1308–1319.

Qu, E., & Frias, R. (2009). Azo-dye Orange II degradation by Fenton ' s reaction using Fe / ZSM-5 zeolite as catalyst, (II), 72-98.

Ramirez, H., Costa, C., & M. Madeira, L. (2005). Experimental design to optimize the degradation of the synthetic dye Orange II using Fenton's reagent. Catalysis Today, 107, 68–76.

Rey, A., Faraldos, M., Casas, J. A., Zazo, J. A., & Bahamonde, A. (2009). Applied Catalysis B : Environmental Catalytic wet peroxide oxidation of phenol over Fe / AC catalysts : Influence of iron precursor and activated carbon surface, 86, 69–77.

Rodgers-Gray, T. P., Jobling, S., Morris, S., Kelly, C., Kelly, C., Kirby, S., J., & A., Harries, J. E., Waldock, M. J., Sumpter, J. P., & Tyler, C. R. (2000). Long-Term Temporal Changes in the Estrogenic Composition of Treated Sewage Effluent and Its Biological Effects on Fish. Environmental Science and Technology, 34, 1521–1528.

Rodrigues, C. S. D., Soares, O. S. G. P., Pinho, M. T., Pereira, M. F. R., & Madeira, L. M. (2017). p-Nitrophenol degradation by heterogeneous Fenton's oxidation over activated carbon-based catalysts. Applied Catalysis B: Environmental, 219, 109–122.

Rossi, A. F. (2014). Fenton's Process Applied to Wastewaters Treatment, Heterogeneous and Homogeneous Catalytic Operation Modes. University of Coimbra, 67 - 89.

Routledge, E. J. & Sumpter. (2005). Endocrine Disrupters in the Aquatic Environment: An Overview. Acta Hydrochimica et Hydrobiologica, 31 (8), 9–16.

Sanches, S., Barreto, M. T., & Pereira, V. J. (2010). Drinking water treatment of priority pesticides using low pressure UV photolysis and advanced oxidation processes. Water Research, 44(6), 1809–1818.

Sánchez, L., Peral, J., & Domènech, X. (1998). Aniline Degradation by Combined Photocatalysis and Ozonation. Applied Catalysis B: Environmental, 19, 59–65.

Sboui, M., Nsib, M. F., Rayes, A., Swaminathan, M., & Houas, A. (2017). ScienceDirect TiO 2 – PANI / Cork composite : A new floating photocatalyst for the treatment of organic pollutants under sunlight irradiation, 0, 3–13.

Shah I, Adnan R, Wan Ngah WS, Mohamed N (School of Chemical Sciences, Universiti Sains Malaysia, 11800 Penang, M. . (2015). Iron impregnated activated carbon as an efficient adsorbent for the removal of methylene blue: regeneration and kinetics studies., (1932–6203 (Electronic)).

Sivagami, K., Sakthivel, K. P., & Nambi, I. M. (2017). Advanced oxidation processes for the treatment of tannery wastewater. Journal of Environmental Chemical Engineering, 0–1.

Southworth, B. A., & Voelker, B. M. (2003). Hydroxyl Radical Production via the Photo-Fenton Reaction in the Presence of Fulvic Acid. Environmental Science & Technology, 37(6), 1130–1136.

Stajszczyk P., Kos L., Jozwiak W., and P. J. (2006). Application of Fenton's reagent in detergent separation in highly concentrated water solutions. East. Eur., 14, 114–119.

Szpyrkowicz, L.; Juzzolino, C.; Kaul, S. . (2001). A Comparative Study on Oxidation of Disperse

Dyes By Electrochemical Process, Ozone, Hypochlorite and Fenton Reagent. Wat. Res., 35, 2129–2136.

T. W. Graham-Solomons. (1992). Organic Chemistry. John Wiley & Sons, Inc., New York, (5th ed.), 942.

V. Kavitha, K. P. (2005). Destruction of cresols by Fenton oxidation process. Water Res., 39, 3062 –3072.

Vezzoli, M. (2012). Intrinsic kinetics of titania photocatalysis : Simplified Models for their investigation by, (February).

W. chu, C. Y. Kuan, K. H. chan, and S. K. K. (2005). A study of kinetic modeling and reaction pathway of 2, 4-dichlorophenol transformation by photo fenton like oxidation. Journal of Hazardous Materials, 121, 119–126.

WALLACE, J. M. W. K. ogg C. y. (2001). Phenol 1. The Dow Chemical Co., (9), 1–11.

Zepp, R. G., Faust, B. C., & Hoigne, J. (1992). Hydroxyl radical formation in aqueous reactions (pH 3-8) of iron(II) with hydrogen peroxide: the photo-Fenton reaction. Environmental Science & Technology, 26(2), 313–319.

Zhang, T., Li, C., Ma, J., Tian, H., & Qiang, Z. (2008). Surface hydroxyl groups of synthetic a -FeOOH in promoting OH generation from aqueous ozone : Property and activity relationship, 82, 131–137.

Zhang L., Li P., Gong Z., L. X. (2008). Photocatalytic degradation of polycyclic aromatic hydrocarbons on soil surfaces using TiO2 under UV light. J. of Hazardous Materials, 158, 478–484.

APPENDICES

Appendix A: Bulk Density (BD), acid density, reusability test and kinetic model Calculations and data

A1. Bulk density:

$$\text{Bulk density (BD)} = \frac{\text{weight of the sample (g)}}{\text{volume of the sample (ml)}}$$

$$BD_{AC1} = \frac{0.464g}{1.4ml} = 0.3314\ g/ml$$

$$BD_{AC2} = \frac{0.8705g}{2.6ml} = 0.338\ g/ml$$

$$BD_{AC3} = \frac{1.3617g}{3.6ml} = 0.37825\ g/ml$$

$$BD_{Fe/AC\ 1} = \frac{0.412g}{1.2ml} = 0.3433\ g/ml$$

$$BD_{Fe/AC\ 2} = \frac{0.8396g}{1.6ml} = 0.52475\ g/ml$$

$$BD_{Fe/AC\ 3} = \frac{1.4144g}{2.8ml} = 0.50514\ g/ml$$

$$BD_{Fe/AC-So_3\ 1} = \frac{0.492g}{1.1ml} = 0.4472\ g/ml$$

$$BD\ _{Fe/AC-So_3\ 2} = \frac{0.812g}{1.6ml} = 0.5075\ g/ml$$

$$BD\ _{Fe/AC-So_3\ 3} = \frac{1.5205g}{2.6ml} = 0.585\ g/ml$$

A2. Acid density

Detail calculation of total acid density of AC, Fe/AC, AC-SO_3H and Fe/AC-SO_3H

Total acid density for AC

$$N_{total\ acidity} = 0.01\frac{mol}{L} * 0.04L - 0.01\frac{mol}{L} * 0.00355L$$

$$= 0.0004\ mol - 0.000355 mol$$

$$= 0.000045\ mol$$

$$The\ total\ acidity\ per\ gram\ of\ catalyst\ = \frac{0.000045\ mol}{0.05g} = 0.9\ x\ 10^{-3}\ mol/g$$

$$= 0.9\ mmol/g$$

Total acid density for Fe/AC

$$N_{total\ acidity} = 0.01\frac{mol}{L} * 0.04L - 0.01\frac{mol}{L} * 0.0034L$$

$$= 0.0004\ mol - 0.00034 mol$$

$$= 0.00006\ mol$$

$$The\ total\ acidity\ per\ gram\ of\ catalyst\ = \frac{0.00006\ mol}{0.05g} = 1.2\ x\ 10^{-3}\ mol/g$$

$$1.2\ mmol/g$$

Total acid density for AC-SO_3H

$$N_{total\ acidity} = 0.01\frac{mol}{L} * 0.04L - 0.01\frac{mol}{L} * 0.0019L$$

$$= 0.0004\ mol - 0.00019 mol$$

$$= 0.00021\ mol$$

$$The\ total\ acidity\ per\ gram\ of\ catalyst\ = \frac{0.00021\ mol}{0.05g} = 4.2\ x\ 10^{-3}\ mol/g$$

$$= 4.2\ mmol/g$$

Total acid density for $Fe/AC - SO_3H$

$$N_{total\ acidity} = 0.01\frac{mol}{L} * 0.04L - 0.01\frac{mol}{L} * 0.0012L$$

$$= 0.0004\ mol - 0.00012 mol$$

$$= 0.00028\ mol$$

$$The\ total\ acidity\ per\ gram\ of\ catalyst\ = \frac{0.00028\ mol}{0.05g} = 5.6\ x\ 10^{-3}\ mol/g$$

$$= 5.6\ mmol/g$$

Sample calculation of $-SO_3H$ acid density for $AC - SO_3H$

Volume of 0.01 M $NaOH$ (titrant) (data obtained from the titrate analysis): 3.1 ml

SO3H acidity per gram of the sulfonated activate carbon:

$$(0.01M\ of\ NaOH * 0.0037L) = 0.000031\ mol = 0.031\ mmol$$

$$SO3H\ density\ per\ gram\ of\ catalyst = \frac{0.031mmol}{0.05g} = 0.62\ mmol/g$$

Sample calculation of $-SO_3H$ acid density for $Fe/AC - SO_3H$

Volume of 0.01 M $NaOH$ (titrant) (data obtained from the titrate analysis): 3.7 ml

SO3H acidity per gram of the catalyst

$$(0.01M\ of\ NaOH * 0.0037L) = 0.000037\ mol = 0.037\ mmol$$

$$SO3H\ density\ per\ gram\ of\ catalyst = \frac{0.037mmol}{0.05g} = 0.74\ mmol/g$$

Table A1: Reusability test data

	TOC reduction (%)	
No. of cycle	$Fe/AC - SO_3H$	Fe/AC
1	99.8779	95.798
2	97.548	91.52
3	97.125	89.175
4	96.45	88.96

Kinetic model calculation:

Table A2: Data used for kinetic models

Time (min)	ln TOC/TOCo at 30, 60 and 90 ℃		
	30 ℃	60 ℃	90 ℃
60	2.030537	3.195672	2.117451
150	2.02048	2.88	2.05743
240	2.014351	2.609273	1.830091

From the above kinetic plots the following kinetics model equation are derived for each temperature: (at TOC_o = 565.696 mg/L)

At 30 ℃;

$$slope = -9\ x\ 10^{-5} = -ln(K_1' + K_2')$$

$$= K_1' + K_2' = e^{9\ x\ 10^{-5}} = 1$$

$$intercept = ln\frac{K_1'}{K_2'} = 2.0353$$

$$= \frac{K_1'}{K_2'} = e^{2.0353} = 7.65455$$

$$= K_1' = 7.65455\ K_2'$$

$$K_2' + 7.65455\ K_2' = 8.65455K_2' = 1$$

$$K_2' = \frac{1}{8.65455} = 0.1155$$

$$= K_1' = 7.65455\ x\ 0.1155 = 0.8841$$

The equation then become: $\ln TOC = 8.3732 - \ln t$

At 60 ℃;

$$slope = -0.0033 = -ln(K_1' + K_2')$$

$$= K_1' + K_2' = e^{0.0033} = 1.0033$$

$$intercept = \ ln\frac{K_1'}{K_2'} = 3.3836$$

$$= \frac{K_1'}{K_2'} = \ e^{3.3836} = 29.477$$

$$= \ K_1' = 29.477\ K_2'$$

$$K_2' + \ 29.477\ K_2' = 30.477 K_2' = 1.0033$$

$$K_2' = \frac{1.0033}{30.477} = 0.329$$

$$= K_1' = 29.477\ x\ 0.329 = 0.9704$$

The equation then become: $\ln TOC = 9.72 - \ln(1.0033)t$

At 90 ℃;

$$slope = \ -0.0016 = -ln(K_1' + K_2')$$

$$= K_1' + K_2' = \ e^{0.0016} = 1.0016$$

$$intercept = \ ln\frac{K_1'}{K_2'} = 2.2411$$

$$= \frac{K_1'}{K_2'} = \ e^{2.2411} = 9.40367$$

$$= \ K_1' = 9.40367\ K_2'$$

$$K_2' + \ 9.40367\ K_2' = 10.4.0367 K_2' = 1.0016$$

$$K_2' = \frac{1.0016}{10.40367} = 0.0963$$

$$= K_1' = 9.40367\ x\ 0.0963 = 0.90533$$

The equation then become: $\ln \mathrm{TOC} = 8.58 - \ln(1.0016)\mathrm{t}$

Appendix B: Spectrophotometric Determination of Fe^{2+} Ions Using 1, 10-Phenanthroline

- Standard ferrous solution (10 ppm (10 mg/ dm^3)); prepared as follows.
  - Weigh 0.0702 g of analytical grade ferrous ammonium sulphate hexahydrate [$Fe(NH_4)_2(SO_4)_2.6H_2O$].
  - Quantitatively transfer the weighed sample to a volumetric flask of 1L capacity and add sufficient distilled water to dissolve it.
  - Add 2.5 ml of concentrated sulphuric acid and make up the solution to the mark.
- 1, 10-phenanthroline; prepared by dissolving 100 mg of the reagent in 100 ml of distilled water. The reagent can be stored in a bottle.

PROCEDURE

1. Pipette out 1, 2, 3, 5, 10, 15 and 20 ml of the standard ferrous ion solution into a series of 100 ml standard flasks labelled from 1 to 7.
2. In another flask, labelled 'Sample', take 10 ml of the unknown sample.
3. To another 100 ml standard flask, labelled 'Blank', add about 20 ml of distilled water to prepare the blank solution.
4. To each of the above flasks (standards, sample and blank) add 1ml of hydroxylamine hydrochloride and 5 ml of 1, 10-phenanthroline.
5. Buffer each solution by adding 8 ml of acetic acid / sodium acetate buffer.
6. Allow at least 15 minutes after the addition of the reagents for full color development (The color once developed is stable for hours).
7. Dilute each solution exactly to 100 ml mark with distilled water and mix well.
8. The standard solutions so obtained correspond to 0.1, 0.2, 0.5, 1.0, 2.0, 4.0 and 6.0 ppm respectively. You may label the flasks accordingly.
9. Record the absorption spectrum for the 6.0 ppm standard solution against the reagent blank in the range of 400 – 700 nm.
10. Select the wavelength which gives maximum absorbance (λ_{max}) and record the same under observations. The reported value is 508 nm.
11. Calculate the molar absorption coefficient (ε) of the complex from the molar concentration and path length of the cuvette. Use the relation $A = \varepsilon cb$.

12. Measure the absorbance for all the standard solutions at the wavelength of maximum absorption and record the readings in the column no. 4 of the Observation Table 1.2.
13. Measure and record the absorbance for the 'Sample' also in the same way.
14. Make a plot of absorbance at Y-axis (column 4) vs. concentration of the standard solutions at X-axis (column 3) to get the calibration curve. (The linear region of the curve obeys Beer- Lambert's law and is used for the estimation of unknown samples.)
15. Determine the concentration of the given sample solution with the help of the calibration curve.
16. Calculate the ferrous ions present in the unknown sample solution by accounting for the dilution factor and report the value.

Table B1: Collecting absorbance data for the calibration curve

S. No.	Volume of the standard / sample solution (ml)	Conc. of Fe^{2+} ions (ppm)	Absorbance at λ_{max}= 508nm
1	1	0.1	0.00
2	2	0.2	0.325
3	5	0.5	0.464
4	10	1.0	0.658
5	20	2.0	0.775
6	40	4.0	0.879
7	70	7.0	0.966

Calculation of molar absorption coefficient

The absorbance at the λ_{max} = A = ...

Path length of the sample (cuvette cell length) = b= ..... cm

Concentration of the standard solution = c = 6.0 ppm = 6.0 mg / dm^3

$$\frac{2\ x\ 10^{-3}\ g}{605.85\ g\ mol\ dm^{3}} = 9.9\ x\ 10^{-6} mol\ dm^{-3}$$

Determining the concentration of the ferrous ions in the sample from calibration curve

Plot the value of absorbance of the sample solution on the calibration curve obtained in Fig.1.2 and determine the corresponding concentration value (in ppm). The concentration of ferrous ions in the given sample = (Value obtained from the calibration curve × 10) ppm = ...× 10 ppm = ...ppm

[The factor of ten comes from the fact that we took 10 ml of the sample solution and finally diluted it to 100 ml.]

Iron leachate data and calculation

$$\text{Iron leachate (\%)} = \frac{\text{Iron content before treatment } (Fe_b) - \text{ Iron content before treatment}(Fe_a)}{\text{Iron content before treatement } (Fe_b)} \text{ x } 100\%$$

Table B2: iron leachate with time

		Fe_a(Mg)	
Fe_b(Mg)	Time (min)	Fe/AC	Fe/AC − SO_3H
6.481	0	6.481	6.481
6.481	30	5.50885	5.833
6.481	60	5.444	5.7033
6.481	90	5.444	5.6385
6.481	120	5.31442	5.64
6.481	150	5.26158	5.5737
6.481	180	5.255	5.5741
6.481	210	5.266	5.5724

6.481	240	5.256	5.5732

Table B3: Iron leachate in percent

Time (min)	**Iron leachate**	
	Fe/AC	$Fe/AC-SO_3H$
0	**0**	**0**
30	**15**	**10**
60	**16**	**12**
90	**16**	**13**
120	**18**	**13**
150	**19**	**14**
180	**19**	**14**
210	**19**	**14**
240	**19**	**14**

Appendix C: Phenol determination (Spectrophotometric, manual 4-AAP with distillation)

METHOD #: 420.1 Approved for NPDES (Editorial Revision 1978)

TITLE: Phenolics (Spectrophotometric, Manual 4-AAP with Distillation)

ANALYTE: Phenolics:

INSTRUMENTATION: Spectrophotometer

STORET No.: 32730

1.0 Scope and Application

1.1 This method is applicable to the analysis of drinking, surface and saline waters, domestic and industrial wastes.

1.2 The method is capable of measuring phenolic materials at the 5 µ g/L level when the colored end product is extracted and concentrated in a solvent phase using phenol as a standard.

1.3 The method is capable of measuring phenolic materials that contain more than 50 µ g/L in the aqueous phase (without solvent extraction) using phenol as a standard.

1.4 It is not possible to use this method to differentiate between different kinds of phenols.

2.0 Summary of Method

2.1 Phenolic materials react with 4-aminoantipyrine in the presence of potassium ferricyanide at a pH of 10 to form a stable reddish-brown colored antipyrine dye. The amount of color produced is a function of the concentration of phenolic material.

3.0 Comments

3.1 For most samples a preliminary distillation is required to remove interfering materials.

3.2 Color response of phenolic materials with 4-amino antipyrine is not the same for all compounds. Because phenolic type wastes usually contain a variety of phenols, it is not possible to duplicate a mixture of phenols to be used as a standard. For this reason phenol has been selected as a standard and any color produced by the reaction of other phenolic compounds is reported as

phenol. This value will represent the minimum concentration of phenolic compounds present in the sample.

4.0 Sample Handling and Preservation

4.1 Biological degradation is inhibited by the addition of 1 g/L of copper sulfate to the sample and acidification to a pH of less than 4 with phosphoric acid. The sample should be kept at 4°C and analyzed within 24 hours after collection.

5.0 Interference

5.1 Interferences from sulfur compounds are eliminated by acidifying the sample to a pH of less than 4 with H PO4 and aerating briefly by stirring and adding3 CuSO .4

5.2 Oxidizing agents such as chlorine, detected by the liberation of iodine upon acidification in the presence of potassium iodide, are removed immediately after sampling by the addition of an excess of ferrous ammonium sulfate (7.10). If chlorine is not removed, the phenolic compounds may be partially oxidized and the results may be low.

6.0 Apparatus

6.1 Distillation apparatus, all glass consisting of a 1 liter pyrex distilling apparatus with Graham condenser.

6.2 pH meter.

6.3 Spectrophotometer, for use at 460 or 510 nm.

6.4 Funnels.

6.5 Filter paper.

6.6 Membrane filters.

6.7 Separatory funnels, 500 or 1,000 mL.

6.8 Nessler tubes, short or long form.

7.0 Reagents

7.1 Phosphoric acid solution, 1 + 9: Dilute 10 mL of 85% H PO to 100 mL with3 4 distilled water.

7.2 Copper sulfate solution: Dissolve 100 g CuSO4• 5H O in distilled water and 2 dilute to 1 liter.

7.3 Buffer solution: Dissolve 16.9 g NH Cl in 143 mL conc. NH OH and dilute to 250 mL with distilled water. Two mL should adjust 100 mL of distillate to pH 10.

7.4 Aminoantipyrine solution: Dissolve 2 g of 4AAP in distilled water and dilute to 100 mL.

7.5 Potassium ferricyanide solution: Dissolve 8 g of K Fe (CN) in distilled water3 6 and dilute to 100 mL.

7.6 Stock phenol solution: Dissolve 1.0 g phenol in freshly boiled and cooled distilled water and dilute to 1 liter. 1 mL = 1 mg phenol.

7.7 Working solution A: Dilute 10 mL stock phenol solution to 1 liter with distilled water. mL = 10 µg phenol.

7.8 Working solution B: Dilute 100 mL of working solution A to 1000 mL with distilled water. 1 mL = 1 µ g phenol.

7.9 Chloroform

7.10 Ferrous ammonium sulfate: Dissolve 1.1 g ferrous ammonium sulfate in 500 mL distilled water containing 1 mL conc. H SO and dilute to 1 liter with 2 4 freshly boiled and cooled distilled water.

8.0 Procedure

8.1 Distillation

8.1.1 Measure 500 mL sample into a beaker. Lower the pH to approximately 4 with 1 + 9 H PO (7.1), add 5 mL CuSO solution (7.2) and transfer to 3 44 the distillation apparatus. Omit adding H PO and CuSO if sample was2 4 4 preserved as described in 4.1.

8.1.2 Distill 450 mL of sample, stop the distillation, and when boiling ceases add 50 mL of warm distilled water to the flask and resume distillation until 500 mL have been collected.

8.1.3 If the distillate is turbid, filter through a prewashed membrane filter.

8.2 Direct photometric method

8.2.1 Using working solution A (7.7), prepare the following standards in 100 mL volumetric flasks.

Direct photometric method

8.2.1 Using working solution A (7.7), prepare the following standards in 100 mL volumetric flasks.

8.2.2 To 100 mL of distillate or an aliquot diluted to 100 mL and/or standards, add 2 mL of buffer solution (7.3) and mix. The pH of the sample and standards should be 10 ± 0.2.

8.2.3 Add 2.0 mL aminoantipyrine solution (7.4) and mix.

8.2.4 Add 2.0 mL potassium ferricyanide solution (7.5) and mix.

8.2.5 After 15 minutes read absorbance at 510 nm.

Accordingly, calibration curve was employed for calculation of phenol concentration. Based on calibration curve (fig. --) 'm' value of 1.74 indicates a fit linear correlation. Equation 4.1 is developed from calibration curve was used to calculate phenol concentration in unknown samples. The full UV spectrum of standard phenol solution (solvent: distilled water)

Table C1: Calibration curve data of phenol solution

Label	Absorption (270 nm)	Concentration (mg/L)
0	0.00	0.00
1	0.224	12.68
2	0.455	25.36
3	0.686	38.04
4	0.876	50.072

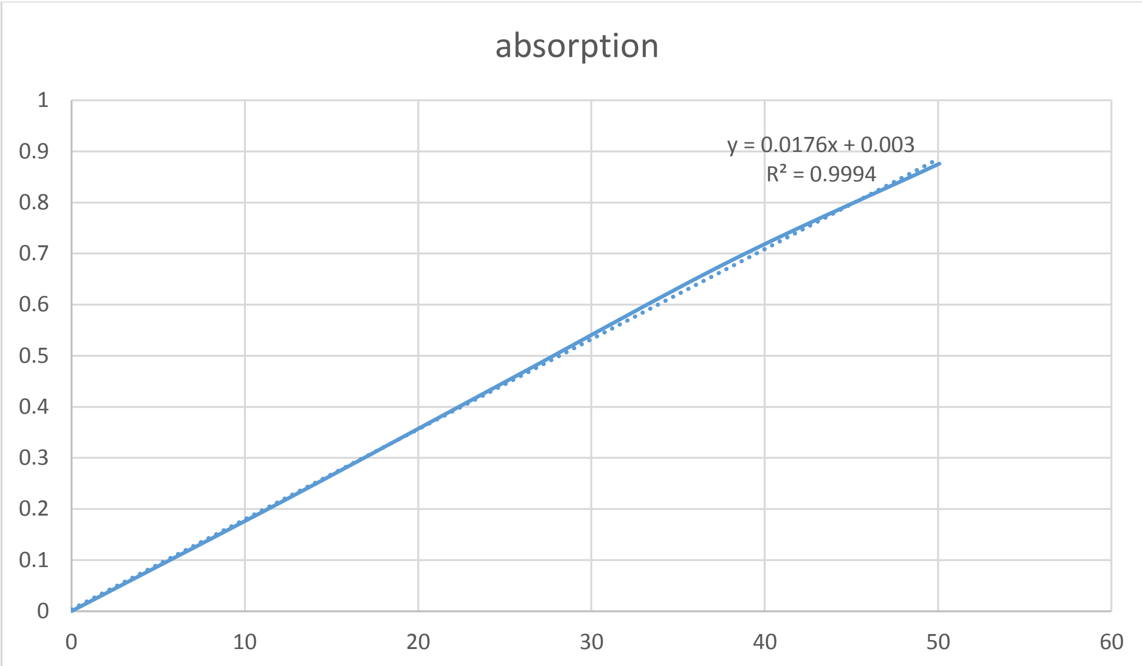

Figure C 1: Calibration curve of phenol solution

b= 0.003006

Slope (m) = 0.017645

$$y = mx + b$$

where: $y = \text{absoption}$

$x = \text{concentration}$

$m = \text{slope}$

$b = \text{intercept}$

$$y = 0.017645x + 0.003006 \ldots\ldots\ldots\ldots\ldots\ldots\ldots\ldots\ldots\ldots\ldots\ldots\ldots\ldots\ldots\ldots\ldots\ldots\ldots\ldots\ldots\ldots\ldots\ldots\ldots\ldots 4.1$$

Table C2: Absorbance reading from UV-Vis spectrophotometry

Number of samples	Absorbance reading		
	AC	Fe/AC	$Fe/AC - SO_3H$
1	0.226	0.823	0.996

2	0.303	0.756	0.974
3	0.234	0.812	1.033

Since initial phenol concentration = 800 mg/L

For phenol adsorbed by AC =Z1;

$$0.226 = (0.017645 * x) + 0.003006$$

$$0.222994 = 0.017645 * x$$

$$x = 12.6378011 \frac{mg}{L}$$

$$= 12.6378011 * 10 = 126.378011 \frac{mg}{L}$$

$$Z_1 = 800 \frac{mg}{L} - 126.378011 \frac{mg}{L} = 673.622 \frac{mg}{L}$$

$$\%Z_1 = \frac{800 - 673.622}{800} = 84.203\%$$

For phenol adsorbed by Fe/AC=Z2;

$$0.823 = (0.017645 * x) + 0.003006$$

$$0.819994 = 0.017645 * x$$

$$x = 46.47175 \frac{mg}{L}$$

$$= 46.47175 * 10 = 464.7175 \frac{mg}{L}$$

$$Z_1 = 800 \frac{mg}{L} - 464.7175 \frac{mg}{L} = 335.2825 \frac{mg}{L}$$

$$\%Z_1 = \frac{800 - 335.2825}{800} = 58.09\%$$

For phenol adsorbed by $Fe/AC - SO_3H$ =Z3

$$0.996 = 0.017645x + 0.003006$$

$$0.993 = 0.017645x$$

$$x = 56.276225 \frac{mg}{L}$$

$$= 56.276225 * 10 = 562.76225 \frac{mg}{L}$$

$$\% \text{ of } Z_2 = \frac{800 - 562.76225}{800} = 29.66\%$$

Accordingly concentration of the materials are calculated and the average percentage was then shown on table 4.6.

Table C3: D- Optimal experiment for pH optimization and catalyst selection

Std.	Type of catalyst.	pH	Total phenol removal (%)	TOC reduction (%)
1	Fe/AC	3.00	83.11	68.75
2	Fe/AC-SO3H	3.00	96.15	91.712
3	Fe/AC	3.75	98.61	90.45
4	Fe/AC-SO3H	3.75	99.13	97.103
5	Fe/AC	4.50	89.73	45.01
6	Fe/AC-SO3H	4.50	95.8	78.45
7	Fe/AC	5.25	85.94	33.22
8	Fe/AC-SO3H	5.25	90.33	53.25
9	Fe/AC	6.00	70.57	21.05
10	Fe/AC-SO3H	6.00	75.33	50.65

Table C4: data of TOC readings and TOC adsorbed

TOC inintial	TOC Adsorbed By the $Fe/AC-SO_3H$	Untreated TOC	TOC final
800	234.4040805	565.5959195	78.47304
800	234.4040805	565.5959195	21.97962
800	234.4040805	565.5959195	80.64663
800	234.4040805	565.5959195	74.24295
800	234.4040805	565.5959195	23.15493
800	234.4040805	565.5959195	68.06268
800	234.4040805	565.5959195	76.09528
800	234.4040805	565.5959195	48.69724
800	234.4040805	565.5959195	131.6928
800	234.4040805	565.5959195	58.50015
800	234.4040805	565.5959195	10.80458
800	234.4040805	565.5959195	90.08925
800	234.4040805	565.5959195	50.31881
800	234.4040805	565.5959195	3.372648
800	234.4040805	565.5959195	72.27298
800	234.4040805	565.5959195	78.71229
800	234.4040805	565.5959195	31.98558
800	234.4040805	565.5959195	120.6869
800	234.4040805	565.5959195	104.948
800	234.4040805	565.5959195	58.63024
800	234.4040805	565.5959195	119.1004
800	234.4040805	565.5959195	75.45445
800	234.4040805	565.5959195	41.62107
800	234.4040805	565.5959195	90.72102
800	234.4040805	565.5959195	81.74841
800	234.4040805	565.5959195	68.88902
800	234.4040805	565.5959195	120.8554
800	234.4040805	565.5959195	19.19689
800	234.4040805	565.5959195	6.336937
800	234.4040805	565.5959195	16.28916
800	234.4040805	565.5959195	32.93182
800	234.4040805	565.5959195	24.91676

Appendix D: Infrared Spectroscopy Correlation Table

Table D1: Infrared Spectroscopy Correlation

Bond	Type of bond	Specific type of bond	Absorption peak (cm^{-1})	Appearance
C—H	Alkyl	Methyl	1260	Strong
			1380	Weak
			2870	medium to strong
			2960	medium to strong
		methylene	1470	Strong
			2850	medium to strong
			2925	medium to strong
		methine	2890	Weak
	vinyl	$C{=}CH_2$	900	Strong
			2975	medium
			3080	medium
		C═CH	3020	medium
		monosubstituted alkenes	900	Strong
			990	Strong
		cis-disubstituted alkenes	670–700	Strong
		trans-disubstituted alkenes	965	Strong
		trisubstituted alkenes	800–840	strong to medium
	aromatic	Benzene /sub. Benzene	3070	Weak
		monosubstituted benzene	700–750	Strong
			690–710	Strong
		ortho-disub. Benzene	750	Strong
		Meta-disub. Benzene	750–800	Strong
			860–900	Strong
		Para-disub. Benzene	800–860	Strong
	alkynes	Any	3300	Medium
	aldehydes	Any	2720	Medium

Bond	Type of bond	Specific type of bond	Absorption peak (cm^{-1})	Appearance
			2820	
C═C	acyclic C═C	monosub. alkenes	1645	Medium
		1, 1-disub. alkenes	1655	Medium
		Cis - 1, 2-disub. Alkenes	1660	Medium
		Trans- 1, 2-disub. Alkenes	1675	Medium
		trisub, tetrasub. Alkenes	1670	Weak
	conjugated C═C	Dienes	1600	Strong
			1650	Strong
	with benzene ring		1625	Strong
	with C═O		1600	Strong
	C═C (both sp^2)	Any	1640–1680	Medium
	aromatic C═C	Any	1450	weak to strong (usually 3 or 4)
			1500	
			1580	
			1600	
	C≡C	terminal alkynes	2100–2140	Weak
		disubst. alkynes	2190–2260	very weak (often indistinguishable)
C=O	aldehyde/ketone	saturated aliph./cyclic 6-membered	1720	
		α,β-unsaturated	1685	
		aromatic ketones	1685	
		cyclic 5-membered	1750	
		cyclic 4-membered	1775	
		aldehydes	1725	influenced by conjugation (as with ketones)
	carboxylic acids/derivates	saturated carboxylic acids	1710	
		unsat./aromatic carb. acids	1680–1690	
		esters and lactones	1735	influenced by conjugation and ring size (as with ketones)

Bond	Type of bond	Specific type of bond	Absorption peak (cm^{-1})	Appearance
		anhydrides	1760	
			1820	
		acyl halides	1800	
		amides	1650	associated amides
		carboxylates (salts)	1550–1610	
		amino acid zwitterions	1550–1610	
O─H	alcohols, phenols	low concentration	3610–3670	
		high concentration	3200–3400	Broad
	carboxylic acids	low concentration	3500–3560	
		high concentration	3000	Broad
N─H	primary amines	Any	3400–3500	Strong
			1560–1640	Strong
	secondary amines	Any	>3000	weak to medium
	ammonium ions	Any	2400–3200	multiple broad peaks
C─O	alcohols	Primary	1040–1060	strong, broad
		secondary	~1100	Strong
		Tertiary	1150–1200	Medium
	phenols	Any	1200	
	ethers	aliphatic	1120	
		aromatic	1220–1260	
	carboxylic acids	Any	1250–1300	
	esters	Any	1100–1300	two bands (distinct from ketones, which do not possess a C─O bond)
C─N	aliphatic amines	Any	1020–1220	often overlapped
	C═N	Any	1615–1700	similar conjugation effects to C═O
	C≡N (nitriles)	unconjugated	2250	Medium
		conjugated	2230	Medium
	R─N─C (isocyanides)	Any	2165–2110	
	R─N═C═S	Any	2140–1990	
C─X	fluoroalkanes	Ordinary	1000–1100	
		trifluromethyl	1100–1200	two strong, broad bands

Bond	Type of bond	Specific type of bond	Absorption peak (cm^{-1})	Appearance
	chloroalkanes	Any	540–760	weak to medium
	bromoalkanes	Any	500–600	medium to strong
	iodoalkanes	Any	500	medium to strong
N─O	nitro compounds	aliphatic	1540	Stronger
			1380	Weaker
		aromatic	1520	lower if conjugated
			1350	
P─C	Organophosphorus compound	aromatic	1440-1460	Medium
P─O	phosphorus oxide	Bonded	1195-1250	Strong
		Free	1250-1300	Strong

Source: (http://en.wikipedia.org/wiki/Infrared_spectroscopy_correlation_table)

Appendix E: Design expert run data

Table E1: Predicted and experimentally obtained values

Std.	Temperature (°C)	Hydrogen peroxide conc. (mg/l)	Time (min)	TOC reduction	Predicted value	Residuals
1	30.00	1000.00	60.00	86.1256	87.29	-1.16
2	60.00	1000.00	60.00	96.1139	95.59	0.53
3	90.00	1000.00	60.00	85.7413	86.17	-0.43
4	30.00	3500.00	60.00	86.8735	89.24	-2.37
5	60.00	3500.00	60.00	95.9061	96.23	-0.32
6	90.00	3500.00	60.00	87.9662	85.50	2.46
7	30.00	6000.00	60.00	86.546	84.68	1.87
8	60.00	6000.00	60.00	91.3901	90.36	1.03
9	90.00	6000.00	60.00	76.7161	78.33	-1.61
10	30.00	1000.00	150.00	89.6569	87.44	2.21
11	60.00	1000.00	150.00	98.0897	95.49	2.60
12	90.00	1000.00	150.00	84.0718	85.82	-1.75
13	30.00	3500.00	150.00	91.1034	90.67	0.44
14	60.00	3500.00	150.00	99.4037	97.41	2.00
15	90.00	3500.00	150.00	87.2218	86.43	0.79
16	30.00	6000.00	150.00	86.0833	87.38	-1.30
17	60.00	6000.00	150.00	94.3448	92.81	1.53

18	90.00	6000.00	150.00	78.662	80.53			-1.87
19	30.00	1000.00	240.00	81.4447	82.12			-0.67
20	60.00	1000.00	240.00	89.6339	89.91			-0.28
21	90.00	1000.00	240.00	78.9425	80.00			-1.05
22	30.00	3500.00	240.00	86.6593	86.62			0.042
23	60.00	3500.00	240.00	92.6412	93.11			-0.46
24	90.00	3500.00	240.00	83.9601	81.88			2.08
25	30.00	6000.00	240.00	85.5465	84.61			0.94
26	60.00	6000.00	240.00	87.8201	89.79			-1.97
27	90.00	6000.00	240.00	78.6322	77.26			1.38
28	60.00	3500.00	150.00	96.6059	97.41			-0.80
29	60.00	3500.00	150.00	98.8796	97.41			1.47
30	60.00	3500.00	150.00	97.12	97.41			-0.29
31	60.00	3500.00	150.00	94.1775	97.41			-3.23
32	60.00	3500.00		150.00	95.5946	97.41	-1.81	

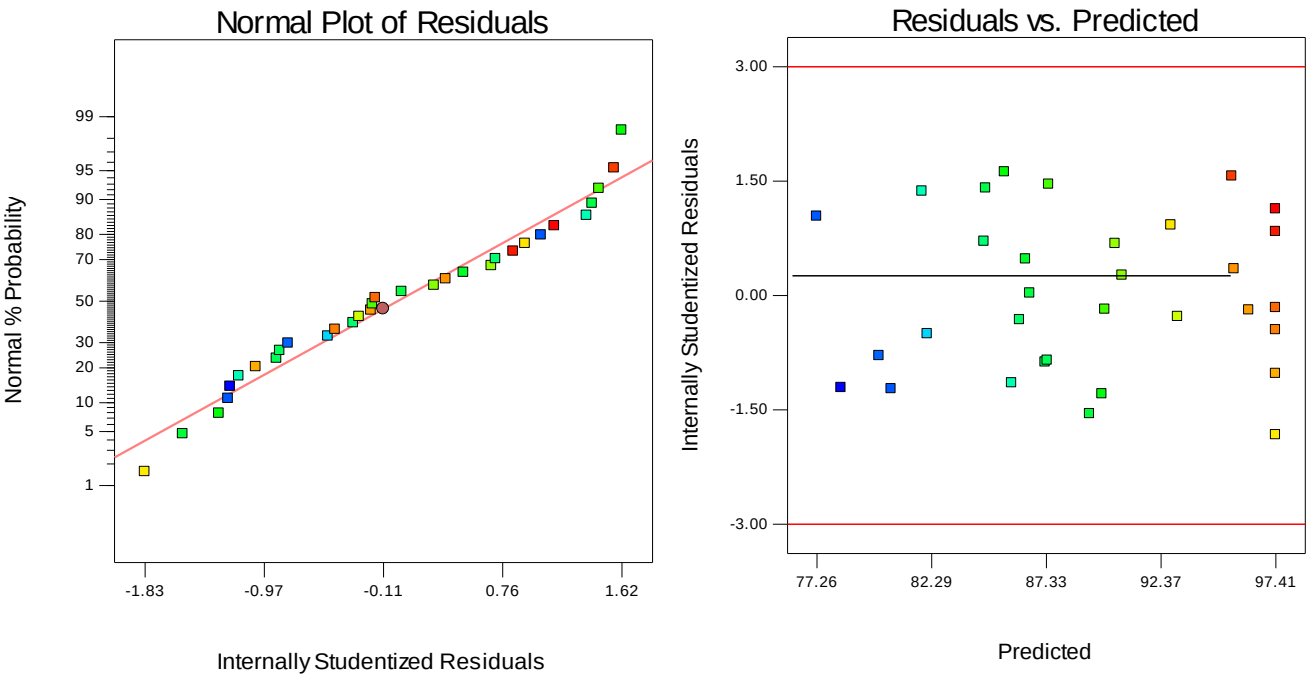

(a) (b)

Figure E1: (a) Normal Plot of residuals and (b) residual vs. predicted

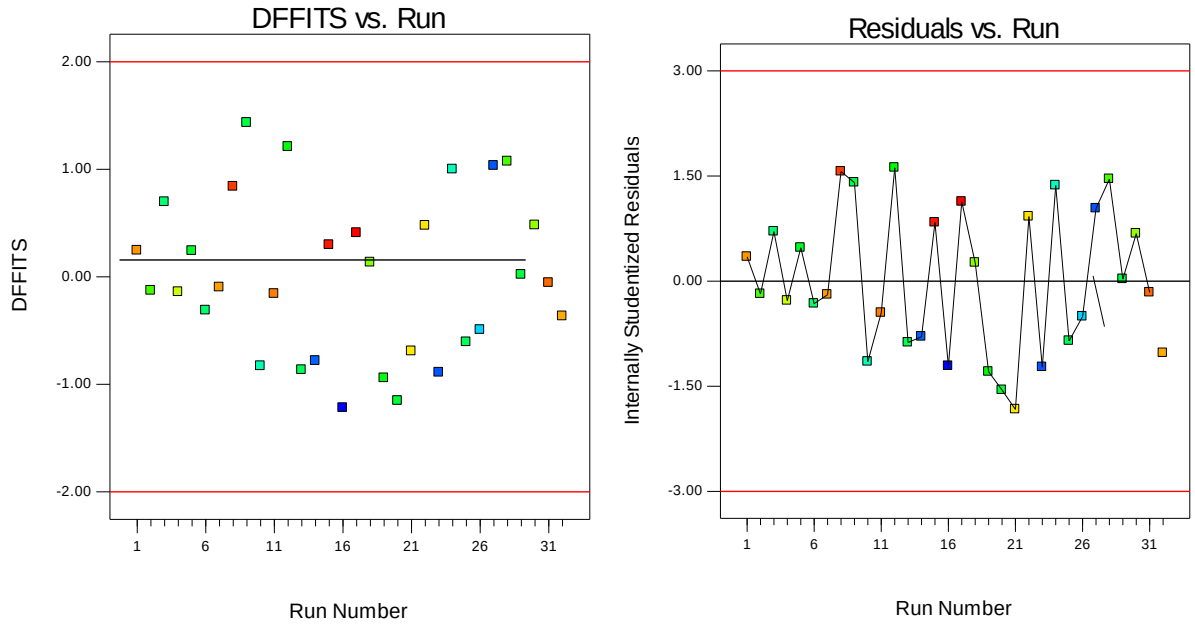

(a) (b)

Figure E2: Plots of (a) DFFITS vs. Run and (b) residual Vs. Run

Table E2: Sequential Model Sum of Squares [Type I] model fittings

Source	Sum of Squares	df	Mean Square	F Value	p-value Prob > F	
Mean vs Total	2.538E+005	1	2.538E+005			
Linear vs Mean	156.83	3	52.28	1.32	0.2883	
2FI vs Linear	40.80	3	13.60	0.32	0.8124	
Quadratic vs 2FI	992.86	3	330.95	94.29	<0.0001	Suggested
Cubic vs Quadratic	32.15	7	4.59	1.53	0.2315	Aliased
Residual	45.07	15	3.00			
Total	2.550E+005	32	7969.93			

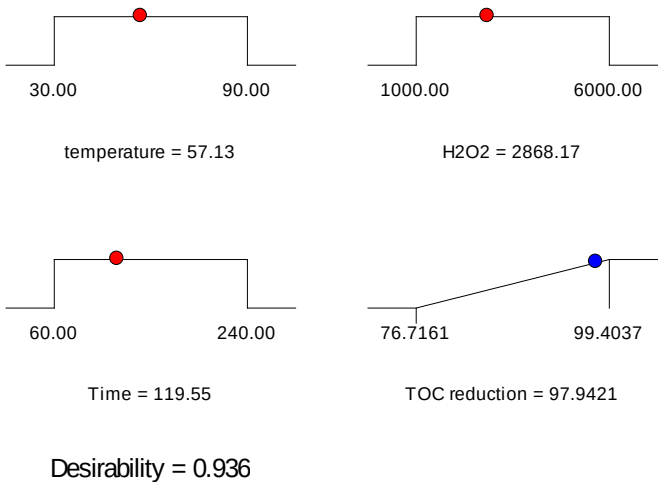

Figure E3: Report of desirability ramps

Appendix F: Laboratory Equipment's and Samples Photo

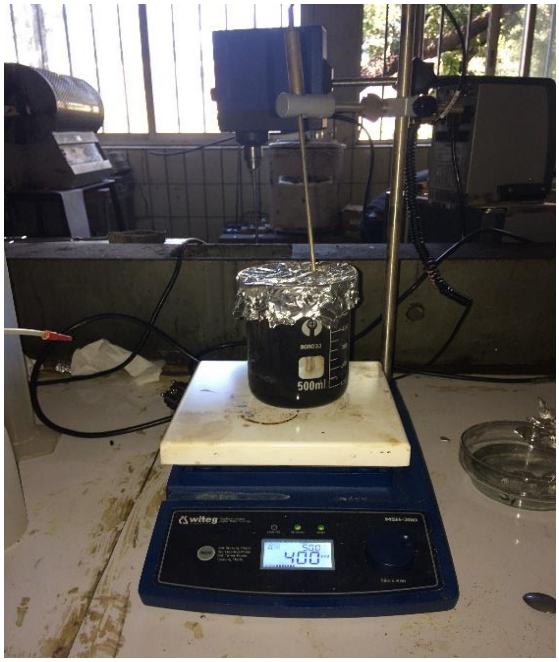

F1: Iron impregnation using MSH-D magnetic stirrer

F2: Sulfonation under nitrogen gas

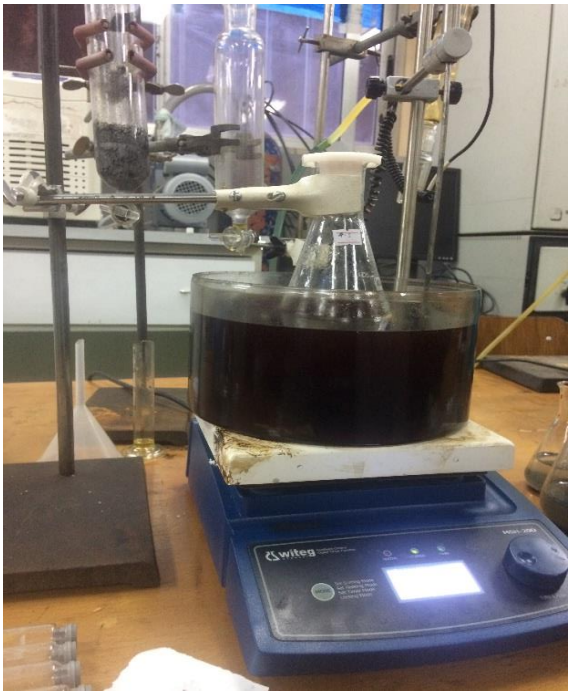

F 3: Catalytic oxidation

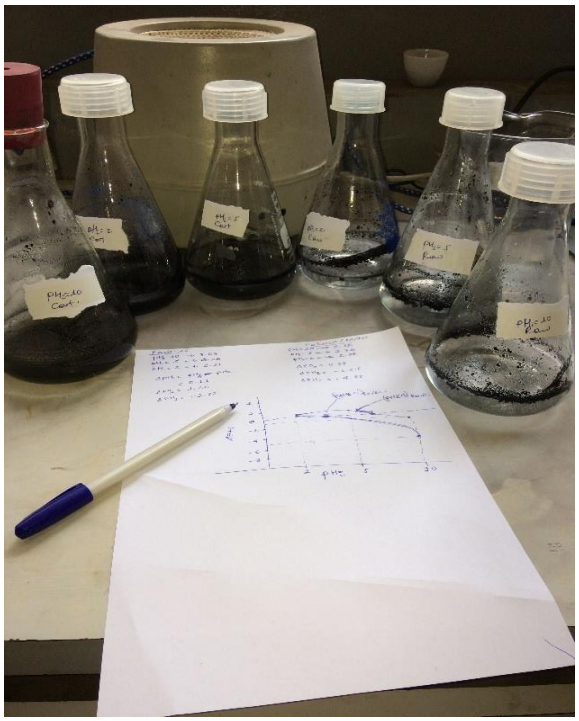

F 4: PHZPC measurement

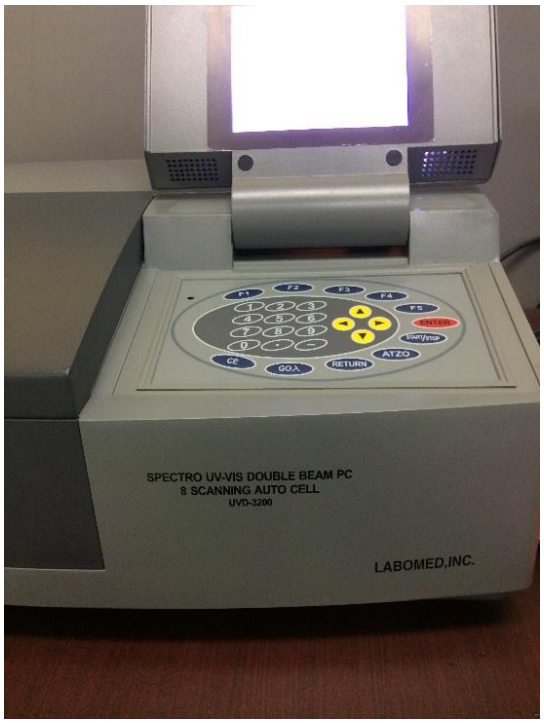

F 5: UV- Vis spectrophotometry instrument

F 6: protection during experiment

F 7: FT-IR instrument

F 8: Solutions used for calibration in TPh determination